Novel bacteriophage-based nanoligands

Marta Sofia Navalho Patinha

Thesis to obtain the Master of Science Degree in

Biotechnology

Supervisors: Professor Ana Margarida Nunes da Mata Pires de Azevedo

Doctor Verónica Martins Romão

Examination Committee

Chairperson: Professor Arsénio do Carmo Sales Mendes Fialho

Supervisor: Doctor Verónica Martins Romão

Members of the Committee: Doctor Sofia de Medina Aires Martins

December 2020

Preface

The work presented in this thesis was performed at the Institute for Bioengineering and Biosciences of Instituto Superior Técnico (Lisbon, Portugal), during the period September-November 2020, under the supervision of Professor Ana Azevedo and Doctor Verónica Romão.

Declaration

I declare that this document is an original work of my own authorship and that it fulfils all the requirements of the Code of Conduct and Good Practices of the Universidade de Lisboa

Acknowledgments

First of all, I would like to thank my supervisors, Professor Ana Azevedo and Doctor Verónica Romão, for giving me the opportunity of working on such a challenging and interesting project. Thank you for all the support, guidance, availability and trust, especially in such a challenging time where this thesis took place.

I would also like to acknowledge all my laboratory colleagues in the 7th and 8th floors, for all the help and support given in the course of this project. I would also like to acknowledge Ana Rita Soares, from INESC-MN, for all the support given, especially during the pandemic period.

A special thanks to João Lampreia, for not only teaching me all about bacteriophages, but specially for all the patience, availability and help you gave me during my thesis. For always maintaining the calm and for all the support given when chaos started to surge on the laboratory. I would like to give a special thank you to my colleague Inês Simões, for being there along the journey that was this master thesis. For all the moments where we shared our success and failures. For all the great and funny moments in the laboratory, that helped endure the most chaotic and stressful moments.

A very special thanks to my friends, for all the friendship and encouragement they gave me, even after my lack of time for them.

Finally, the sincerest thank you to my family, especially my mom, dad and sister. Thank you for all the patience, love and strength you have given me in the most difficult moments, but most importantly, thanks for the endless belief you had in me.

Thank you all!

Resumo

Bacteriófagos são vírus capazes de atacar e infetar bactérias, possuindo grande especificidade para esses organismos. Devido a uma ampla gama de grandes propriedades - alta especificidade, grande robustez, resistência a condições extremamente severas, baixo custo e facilidade de produção - tem havido um interesse crescente no uso de bacteriófagos em eventos de biorreconhecimento. Por outro lado, também tem havido grande interesse na conjugação de moléculas biológicas capazes de direcionar bactérias com nanopartículas. As nanopartículas têm a grande vantagem de permitir a marcação do agente de reconhecimento e, consequentemente, da molécula alvo. No caso das nanopartículas magnéticas, elas têm a vantagem adicional de aumentar o potencial de manipulação das moléculas alvo por meio da captura, sua concentração e deteção magnética. A estratégia de marcação magnética mais comumente usada é feita através da incorporação de nanopartículas que se ligam aleatoriamente no exterior do fago, o que pode levar à perda da capacidade de reconhecimento ou à lise da bactéria alvo antes de sua deteção. O principal objetivo deste projeto é o desenvolvimento de um novo nanoligando baseado em bacteriófagos, onde nanopartículas magnéticas são incorporadas dentro da capsíde do fago, permitindo superar as desvantagens da marcação padrão. Como métodos de conjugação do fago com as MNPs, ambas as estratégias de choque osmótico e sonicação foram aplicadas ao fago T4. Posteriormente, os fagos magnéticos devem ser usados no desenvolvimento de ensaios de deteção magnéticos. Biossensores magnetorresistivos baseados em fagos já estão em desenvolvimento no INESC-MN e sendo explorados para deteção de células bacterianas. No futuro, os fagos magnéticos aqui desenvolvidos serão testados, validados e incorporados como entidades de rotulagem em tais biossensores magnéticos. As perspetivas futuras residem na otimização dos processos de conjugação, bem como na investigação de novas abordagens, na posterior caracterização dos fagos magnéticos por TEM e posteriores testes realizados em biossensores magnéticos desenvolvidos no INESC-MN.

Palavras-chave: Bacteriófagos, Métodos de Detecção de Bactérias, Nanopartículas, Nanopartículas Magnéticas, Magnetófago, Novos Nanoligandos

Abstract

Bacteriophages are viruses that are able to target and infect bacteria, having great specificity to these organisms. Due to a wide range of great properties – high specificity, great robustness, resistance to extremely harsh conditions, low cost and easiness of production – there's been an increasing interest in the use of bacteriophages in biorecognition events. On the other hand, there's also been great interest in the conjugation of biological molecules capable of targeting bacteria with nanoparticles. Nanoparticles have the great advantage of allowing the labelling of the recognition agent and, consequently, the target molecule. In case of magnetic nanoparticles, they have the additional advantage of increasing the potential of manipulation of the target molecules through capture, their concentration and magnetic detection. The most commonly used magnetic labelling strategy is done through the incorporation of nanoparticles that bind randomly on the phage exterior, that can lead to loss of recognition capacity or the lysis of the target bacteria before their detection. The main objective of this project is the development of a novel bacteriophage-based nanoligand, where magnetic nanoparticles are incorporated inside the phage capsid, allowing to overcome standard labelling disadvantages. As conjugation methods of phage with the MNPs, both osmotic shock and sonication strategies were applied to T4 phages. Afterwards, the magnetic-phages are to be used in the development of magnetic-based detection assays. Phage-based magnetoresistive biosensors are already under development at INESC-MN and being explored for bacterial cells detection. In the future, the magnetic phages here developed will be tested, validated and incorporated as labelling entities in such magnetic biosensors. Future perspectives lie in the optimization of the conjugation processes, as well as investigation of new approaches, the following characterization of the magnetic phages in TEM and further testing in magnetic biosensors developed in INESC-MN.

Keywords: Bacteriophages, Bacterial Detection Methods, Nanoparticles, Magnetic Nanoparticles, Magnetophage, Novel Nanoligands

Contents

List of Tables

List of Figures

List of Abbreviations

Al_2O_3	Aluminium Oxide
Au	Silver
BARC	Bead Array Counter
BSA	Bovine Serum Albumin
$C_2H_3NaO_2$	Sodium Acetate
CFU	Colony Forming Units
Cr	Chromium
DNA	Deoxyribonucleic Acid
dsDNA	Double-Stranded Deoxyribonucleic Acid
dsRNA	Double-Stranded Ribonucleic Acid
ECA	Enterobacterial Common Antigen
ELISA	Enzyme-Linked Immunosorbent Assay
Fab	Fragment Antigen Binding
Fc	Fragment Crystalline
Fe	Iron
GMR	Giant Magnetoresistance
ICTV	International Committee On Taxonomy Of Viruses
Ig	Immunoglobin
IgNAR	Novel Antigen Receptor
IMS	Immunomagnetic Separation
LOD	Limit Of Detection
LPS	Lipopolysaccharides
$MgCL_2$	Magnesium Cloride
MgO	Magnesium Oxide
$MgSO_4.H_2O$	Magnesium Sulfate Heptahydrate
MNPs	Magnetic Nanoparticles
MOI	Multiplicity Of Infection
mRNA	Messenger RNA
MRSAs	Methicillin-Resistant *Staphylococcus Aureus*
MTJ	Magnetic Tunnel Junctions
NMR	Nuclear Magnetic Resoance
NMWC	Nominal Molecular Weight Cutoff
OD	Optic Density
PCR	Polymerase Chain Reaction
PFU	Plaque Forming Units
POC	Point-Of-Care
RBPs	Receptor-Binding Proteins
RNA	Ribonucleic Acid
scFv	Single-Chain Variable Fragments
sdAbs	Single Domain Antibodies
SELEX	Systematic Evolution Of Ligands By Exponential Enrichment
SM	Saline Magnesium

ssDNA	Single-Stranded Deoxyribonucleic Acid
ssRNA	Single-Stranded Ribonucleic Acid
TEM	Transmission Electron Microscophy
TMR	Tunneling Magnetoresistance
TSA	Trypto-Casein Soy Agar
TSB	Tryptio-Casein Soy Broth
VBNC	Viable but Not-Culturable

1. Introduction

In 1928, Sir Alexander Fleming discovered penicillin, a compound currently used for the treatment of many bacterial infections, triggering the beginning of modern era of antibiotics and, consequently, revolutionizing modern medicine and saving many lives. The treatment of bacterial infections with antibiotics started in the early 1940s. However, although effective against bacteria, the excessive misuse of antibiotics in clinical, agricultural and animal settings lead to a widespread emergence and propagation of bacterial strains resistant to multiple classes of antibiotics due to the development of new mechanisms of resistance to this type of compounds[1–3]. Some examples of these pathogens are methicillin-resistant *Staphylococcus aureus* (MRSAs), vancomycin-resistant *Enterococcus faecium*, carbapenem-resistant *Pseudomonas aeruginosa* and *Acinetobacter baumannii,* and even *Klebsiella pneumoniae* that's resistant to most classes of antibiotics[2]. Due to this emerging resistance to antibiotics and the low rate of new antibiotic discovery, pathogenic bacteria have turned into a huge threat to human health, being a leading cause of morbidity and mortality worldwide, causing millions of deaths and hospitalizations per year and generating a significant high social and economic impact worldwide. The most common sources of these infections are clinical, foodborne, airborne, and/or waterborne, where contaminations originated from these sources represent eternal challenges worldwide in the healthcare systems and food safety and environmental monitoring[4–6]. Hospitals are a natural place for finding pathogenic bacteria where, according to the European Centre for Disease Prevention and Control, 4.1 million patients are affected by healthcare-associated bacterial infections each year in Europe alone. The additional costs for the treatment of hospital-related infections are very costly, being estimated to be around 7.5€ billion in Europe and 5$ billion in the United States[7,8]. Additionally, the food industry is also highly susceptible to bacterial contamination. In 2005, 1.8 million people died worldwide due to the consumption of contaminated food and water, and the number of infections and illnesses originating in food reaches 76 million per year in the US alone. From those infections, 325 000 people are admitted to hospitals and 5200 of those infections are lethal[7,9]. This led to the need for a search for not only new methods of treatment but also for fast and reliable detection and identification methods of bacteria.

Nowadays, conventional methods used for bacteria detection are dependent on the culturing and isolation of the target bacteria followed by biochemical confirmation. Although quite cheap and straightforward, the conventional procedure is very time-consuming, having repercussions not only in healthcare but also in industry and security. Therefore, new detection methods are being introduced in the last few years. Among them are nucleic-acid-based (includes PCR and DNA micro-arrays), immune-based methods (includes ELISA and lateral flow immunoassays) and even mass spectrometry[2,7,10].

However, all of them have drawbacks, such as the need for specialized equipment, for trained users and the expensive cost. So, there is a great need for the development of cheap, fast, specific, and sensitive diagnostic approaches for the detection of pathogenic bacteria detection. In response to this problem, there has been a rising interest in bioligands in biomolecular recognition events and the development of affinity-dependant assays.

Bacteriophages are viruses that specifically target and infect bacteria, posing great advantages, such as great specificity, robustness, resistance to harsh conditions and cheap preparation, making them a great candidate not only for phage-therapy but also as biorecognition element in affinity-dependant assays. On the other hand, magnetic nanoparticles have been attracting much interest as a labelling material for advanced biological and medical applications, such as biomagnetic concentration and separation, drug delivery, magnetic resonance imaging, and hyperthermia. In this thesis, it will be explored the combination of both, bacteriophages and magnetic nanoparticles, in the development of new detection tools for bacteria.

2. State of the Art

2.1. Bacteriophages as Biorecognition Elements:

Biorecognition molecules are able to recognize and interact with high specificity with a target analyte and are a key component in the development of biosensors, determining the efficiency of the biosensor in terms of both sensitivity and specificity. The choice of the biorecognition element is highly dependent on the target analyte, since in the case of bacterial detection, it can be through the recognition of the whole cell or through the detection of some of their components. For the detection of bacterial cell components, such as DNA, RNA (e.g. mRNA), intracellular proteins (e.g. enzymes) and extracellular vesicles, the most commonly used biorecognition elements are enzymes and oligonucleotides. The main disadvantage of the detection of cell components it's the need for sample processing and extra reagents, adding to the time and cost of those tests. On the other hand, whole cell detection is more desirable, being a more direct method of detection and being faster and more affordable. When detecting whole cells, it can avoid the detection of false positives caused by the detection of only cellular debris from dead cells. Additionally, the bacterial DNA can remain present long after an infection has disappeared, also leading to the detection of false positives. Another associated advantage of whole cell detection is that it is also possible to detect VBNC (Viable but Non-Culturable) cells that are not detected in culture methods. The most used recognition elements for this type of tests are antibodies, aptamers and bacteriophages[5].

2.1.1. Antibodies

Antibodies are the main affinity ligand chosen for the detection of pathogens in clinical and food samples. These molecules are a class of glycoproteins, also known as immunoglobins (Ig), that are produced by plasma B-cells in response to the presence of a foreign entity, such as viruses and bacteria. They naturally occur as part of the mammalian immune system and they recognize an unique part of the foreign target, the antigen, and such recognition is based on an affinity-based recognition mechanism[11–13]. They have the general structure of an "Y", comprising two light chains and two heavy chains linked through disulphate bonds, where each chain is divided into a variable region and a constant region. Each antibody is composed by two fragment antigen binding (Fab), which are involved in the binding of the antibody to the antigen, and a fragment crystalline (Fc), which is involved in the binding to a specific Fc receptor (and other components of the immune system) and in the consequent triggering of the immune response[14]. The variable region, containing amino-acid sequences responsible for the antibody affinity and selectivity to specific antigens, is present in the Fab domain, shaping the paratope of the antibody, which will directly interact with the antigen. However, these structures only interact with a small part of the antigen, the epitope, only allowing the formation of an antibody-antigen complex with antigens with the fitting epitope through a "lock and key" fitting mechanism (Figure 1)[11,14–16].

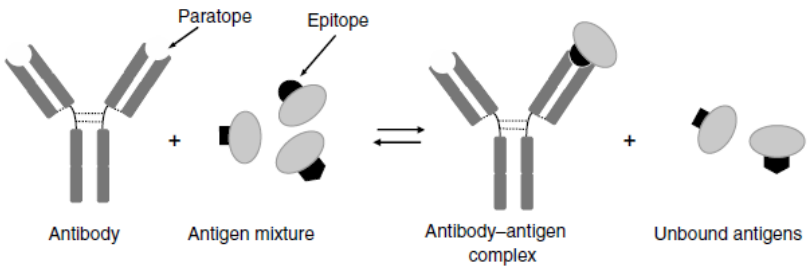

Figure 1 – Schematic representation of the interaction between antibody and antigen[14].

Due to their advantages – adaptability, ease of incorporation into diverse systems and high specificity to their target antigens – they have become the main affinity ligands chosen for the detection of pathogens in clinical and food samples[6,17]. However, there is also a wide range of drawbacks associated to these biorecognition elements. Normally, antibodies are prepared either monoclonal or polyclonal.

Polyclonal antibodies are characterized by having a wide range of specificities, being able to recognize multiple epitopes of one same antigen[18]. This results in a lack of selectivity that is highly disadvantageous for their application in the recognition of specific pathogenic bacteria. On the same note, their use can also result in false positives due to cross-reactivity, since these types of antibodies will be able to detect some of those antigens present in related non-pathogenic organisms that are not the target. Additionally, the production of polyclonal antibodies requires the immunization of animals with multiple injections with a specific antigen and the following harvest (through the serum) and purification of the antibodies, ending up to be very time-consuming and labor-heavy[19,20]. This production process can also result in batch-to-batch variations on the final product, since the injected antigens commonly have multiple epitopes. Additionally, the generation of this type of antibodies creates ethical concerns, going against the efforts made in the last decades to try to replace, reduce or refine animal use in research. Monoclonal antibodies, on the other hand, are only able to recognize a single epitope in a single antigen, resulting in a higher selectivity compared to the previous element[18]. Unlike their polyclonal variants, monoclonal antibodies are produced *ex-vivo* using hybridoma technology. This makes their production in large scales even more expensive and time-consuming than for polyclonal antibodies[19,20]. Additionally, a disadvantage that is present in both types of antibodies is their instability to environmental fluctuations, especially to very harsh conditions (e.g. high temperatures), making them of limited reusability[6,17,19]. With these problems rose the need to enhance antibody performance and reduce their production time and cost, being accomplished by the development of smaller and more stable antibody-derived fragments through molecular engineering. Examples of these antibody-derived fragments include antigen binding fragments (Fabs) and single-chain variable fragments (scFv), where both comprise antigen-binding specificity. scFv, which are smaller and generally more stable than Fabs, however are more prone to dimerization and aggregation due to the presence of polypeptide linker between the variable heavy and light chain[19,21]. Further antibody size reduction has been archived, resulting in single domain antibodies (sdAbs), composed by just one variable domain (light or heavy), however these fragments are prone to form aggregates[21]. A class of non-human antibodies that have been gaining interest along the years are the camelid antibodies, which are found in llamas,

dromedaries, alpacas and camels. These antibodies have an interesting characteristic, since there are heavy-chain antibodies devoid of the light chains, resulting in having one single domain for antigen binding, known as V_{HH} or nanobody. In a similar note, another novel Ig discovered in sharks have been gaining interest due to owning only a heavy variable domain, called novel antigen receptor (IgNAR). These small variants have many advantages, such as improved solubility, higher robustness and higher stability, leading to an increasing interest in their application in biosensing assays[19,21]. However, one of the main disadvantages of these type of antibodies is their type of production, since they still need the immunization of animals. Even though the animals are not sacrificed, the development of nanobodies requires larger, more complicated housing due to the use of larger animals, which can end up increasing the production costs[22].

2.1.2. Aptamers

Aptamers are single stranded nucleic acids of DNA or RNA that are able to fold into specific 3D structures and selectively bind to specific target molecules (Figure 2). They have been gaining popularity in the last few years, especially in the biosensing area, due to their advantageous properties. Their production is mostly done through a combinatorial selection process named systematic evolution of ligands by exponential enrichment (SELEX), which results in a broad range of aptamers that can bind to a wide range of target molecules (ranging from small molecules to whole cells). The cost of their production is much smaller when compared to antibodies since they can be massively synthesized via chemical progresses. These molecules also present a higher stability that other recognition elements (e.g. proteins and antibodies), allowing a higher number of used without losing their biding capacity. Also, they are more robust than antibodies, being able to endure harsher conditions (e.g pH, temperature) and when suffering denaturation, it's reversible[23,24]. The smaller size of these molecules also allows a higher density for immobilization and the binding to epitopes that are not easily accessed by antibodies[23]. The described properties of aptamers make them a promising alternative to antibodies. However, aptamers can suffer from cross-reactivity, since they are able to bind to molecules with a similar structure to those that they are able to recognize[25].

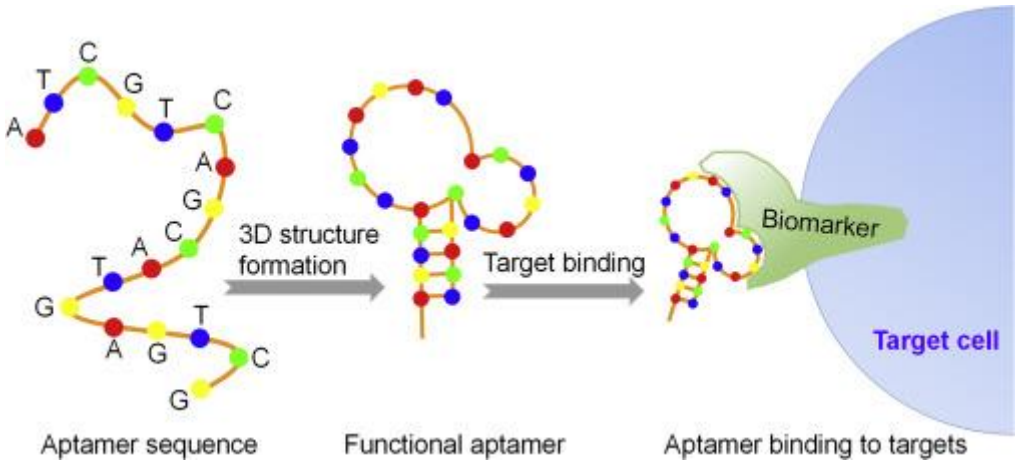

Figure 2 - Schematic representation of the interaction between aptamer and their target[26].

2.1.3. Bacteriophages

Bacteriophages, most commonly known as phages, are viruses that only infect and replicate in bacteria. These viruses are one of the most simple and abundant organisms on Earth and are thought to exist in every ecosystem with an estimated number of 10^{31} phage particles in the biosphere, having a role in the continuous regulation of microbial ecology[27–29]. Since they only affect bacteria, these viruses are harmless to plant, animal and human cells. There's been an increasing interest in the use of bacteriophages in biorecognition events due to their wide range of great properties – being ubiquitous in nature, high specificity, great robustness, resistance to extremely harsh conditions, low cost and easiness of production – allowing the overcoming of the limitations presented by the previous elements[30].

2.1.3.1. Brief History

Bacteriophages were discovered in the beginning of the 20th century independently, both in 1915 by Frederik Twort and then, in 1917, by Felix d'Herelle[31]. Twort discovery took place in the United States, where he observed a small biological entity that destroyed micrococcus colonies in growing cultures, creating a "glassy transformation". He also observed that this "glassy transformation" could be induced in other colonies by its inoculation of the fresh colony, propagating indefinitely[32,33]. d'Herelle discovery took place in France, where he also observed the bacteriophage phenomenon in severe haemorrhagic dysentery. He discovered that these entities were "antagonistic" to bacteria and provoked their lysis in liquid culture and death in the form of clear zones (or "plaques" as he called it) on the agar surface seeded with the bacteria. He termed them as bacteriophages, which means bacteria eater or devour[32,33]. After their discovery, they began to be used as therapeutic agents against infectious diseases, such as *Staphylococcus aureus* and *Bacillus anthracis* infections[34], and as a treatment for typhoid fever and bacillary dysentery[33]. With the advent of World War II and the discovery of antibiotics in the 1940s, the efforts to further study phage therapy decreased significantly in Western Europe and in the United States of America. However, such efforts continued in Eastern Europe and in former Soviet Union[32,35]. In 1940, with the discovery of the electron microscopy, the nature of this microorganism was revealed (Figure 3).

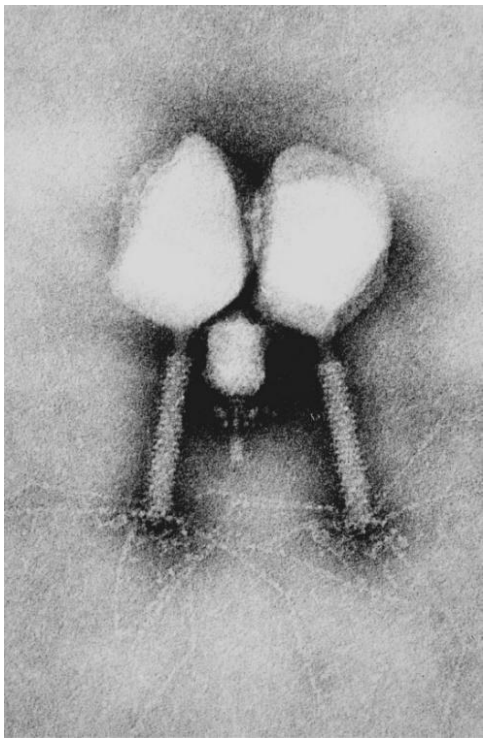

Figure 3 - Electron micrograph of a bacteriophage Φ29 and T2. Adapted from Kutter el al[32].

2.1.3.2. Phage Structure

Phages have a high morphological diversity, however the majorly composed by an icosahedral protein coat, the capsid (also referred to as the “head”), that protects the phage genome, and a tail (Figure 4). The genome can be composed of either DNA or RNA. The head can vary in size and form, going from a hexagonal form to complex structures. The heads are composed by multiple copies of proteins (a single protein or different proteins) and have a very stable organization. Most phages also possess a tail. The bacteriophage tail is linked to the capsid through a connector, which will serve as an adaptor between these two components. The connector is composed by several proteins organized in a helical symmetry and carries out many functions during the phage life cycle (e.g. the packaging of the genomic DNA into the capsid; as the function of gatekeeping the phage DNA, preventing the leakage of it under high pressure and, later, allowing its release into the bacterial host)[36]. The tail attached to the capsid is responsible for host recognition, attachment, and penetration of the cell envelope. This phage component is a hollow tube that connects the phage capsid to the host cell and allows the passage of viral nucleic acids to the host-cell cytoplasm during infection. The tail has tail fibers, attached at the base place, that serves as a recognition agent, due to receptor-binding proteins, for the detection of the target host cell. The tails themselves can also be very diverse, going from being short to long, where the latter can also be divided into contractile or non-contractile[36,37].

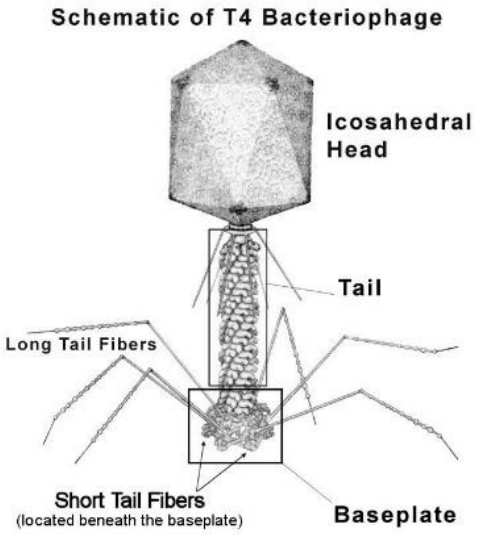

Figure 4 - Graphic representation of a T4 bacteriophage[38].

2.1.3.3. Phage Classification

Bacteriophages present high diversity among themselves, being classified by the International Committee on Taxonomy of Viruses (ICTV). The ICTV presently classifies 14 orders, 150 families, 79 sub-families, 1019 genera and 5560 species[39]. This classification is based on several factors, such as their host preference, morphology type, the environment where they can mostly be found, genome type, mode of infection and auxiliary structures the phage processes, such as tails or envelopes[29,31,36]. Regarding phage morphology and structure, they can be divided into tailed phages, non-tailed icosahedral phages, filamentous phages and pleomorphic phages. They can also be divided into phages that contain a lipid-based envelope or that contain lipids in the particle shell[36]. Regarding the classification based on genome characteristics, as mentioned above, they can be composed of either DNA or RNA. The most common genome among phages is double-stranded DNA (dsDNA), however a small phage group can have single-stranded DNA (ssDNA), single-stranded RNA (ssRNA) or double-stranded RNA (dsRNA)[36]. The genome can range in size from a few to several 100 kb[40]. Additionally, the phages genomes can also either be segmented or non-segmented[35]. They can also be divided into two groups based on their mode of infection, where they can be virulent by performing a lytic infection, or temperate by performing a lysogenic infection, as explained more in depth later in this review[36]. The classification of the bacteriophages could also be regarding their tail type, which has been described previously, can be very diverse. Until 2006, more than 5500 bacteriophages have been examined through electron microscopy, where 96% were tailed phages (classified in the order of *Caudovirales*), being the most predominant against 3.6% of polyhedral, filamentous, and pleomorphic phages[41]. Since *Caudovirales* represents the biggest population of bacteriophages, they are one of the most studied family both biochemically and structurally and one with more practical applications[36]. They are composed by a linear dsDNA genome, a capsid and a tail. The capsid is composed of many copies of the same protein or of a different one, and the corners of the head are made up from pentamers of a

protein and the rest of each side is made up of hexamers of the same or a similar protein. They are also composed approximately by half double-stranded DNA and half protein by mass and their capsid is most commonly icosahedral. *Caudovirales* can be divided into three main families (Figure 5): *Syphoviridae* (A)*, Myoviridae* (B) and *Podoviridae* (C). The *Syphoviridae* family, represented by 60% of tailed phages, is characterized by having non-contractile long and flexible tail. The *Myoviridae* family, represented by 25% of tailed phages, is characterized by phages that have a double-layered contractile tail. The *Podoviridae* family, represented by 15% of tailed phages, is characterized by having very short and stubby tails[32,42].

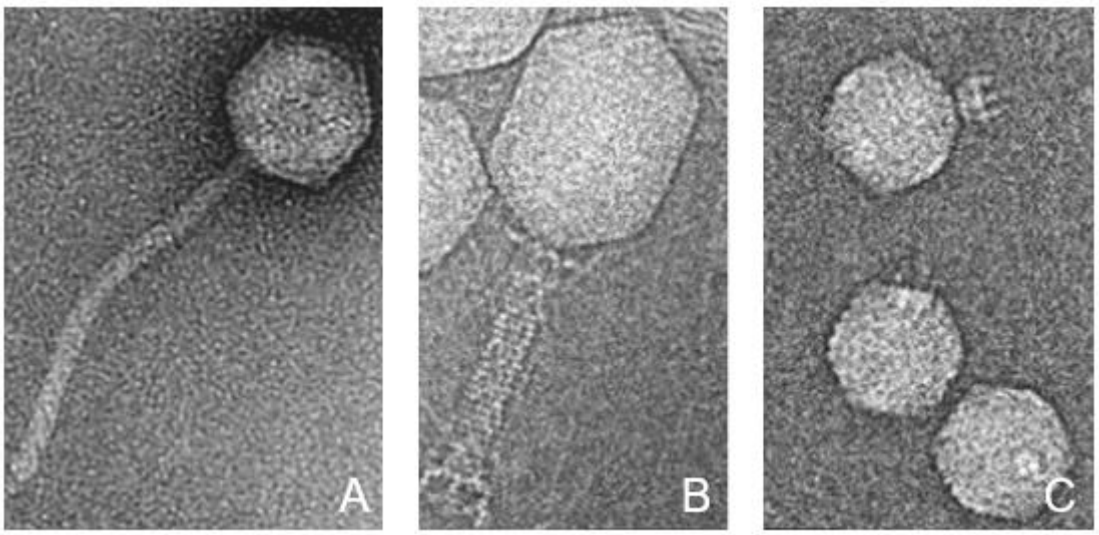

Figure 5 - Transmission Electron Microscopy (TEM) of bacteriophages from the order Caudovirales. Bacteriophages from all three main families are representated: **(A)** Siphoviridae (Phage SPP1), **(B)** Myoviridae (Phage T4) and **(C)** Podoviridae (Phage P22). Adapted from Kurtböke[43].

According to the ICTV page, the *Caudovirales* order has two additional families associated, the *Herelleviridae* and the *Ackermannviridae*, that have been recently discovered. The phages that are not tailed are incorporated in the remaining 3.6% corresponding to polyhedral, filamentous, and pleomorphic phages, not being relevant for this project.

2.1.3.4. Bacteriophage Lifecycle

As mentioned previously, phages can be classified according to their life cycle, i.e. the interaction between phage and host bacteria. Phages can either undergo a lytic cycle, being classified as virulent, or undergo a lysogenic cycle, being classified as temperate. The lytic cycle is divided into five different stages: adsorption, infection, maturation and release. In the adsorption phase, the first interaction between the phage and the bacteria, where the tail recognizes receptors on the bacteria cell wall (also present in the pili or flagella), allowing the phage adsorption and, consequently, the injection of the phage genome into the bacteria. In the majority of phage groups, during the injection step, the capsid and the tails remain in the outside and only the nucleic acids enter the host cell. From this moment, the infection period begins. This period is also known as a latent period, where the bacteriophages assume all the activity of the host cell and take advantage of the bacterial synthetic

machinery, allowing not only the replication of their genetic material but also the production and assembly of new viral components (e.g. capsid and tails). The assembly of new phages is called maturation. The phage components will self-assemble, assembling spontaneously or with the help of specific enzymes. At last, in order to release newly assembled phages, phage produce hydrolytic enzymes (endolysins) that digest the cell wall, weakening it enough so that the internal cell osmotic pressure results in cell lysis. After the release of the new phages into the extracellular space, successive infections of other nearby host bacteria will occur in a rapid and exponential pattern. Productive infections result in the release of up to 1000 progeny phages per infected cell, depending on the type of phage and the cell growth conditions[32,35,36,44,45]. Some examples of virulent bacteriophages are T4, T7, T3 and MS2[46]. A schematic representation of the lytic cycle is presented in Figure 4. The majority of phages are temperate and can follow two replicative models, either following a lytic pathway and lysing the cell or enter the host cell without killing it. In the lysogenic life cycle, the phage DNA is integrated into the host cell chromosome or maintained as a plasmid, being named a prophage. The phage genome persists in a latent state inside the host cell, replicates along with the cell DNA, and being passed to the daughter cells. This process could occur through a great number of generations of bacteria without metabolic consequences. However, if this equilibrium breaks down, due to stress or cellular damage processes of the bacterial host, the bacteriophage (and after excision from the bacterial genome) starts being produced as in a lytic cycle. The host cell start being known as lysogenic or lysogenized, since they possess the ability to induce lysis and the subsequent release of new virions[32,35,36,44,45]. An example of a temperate phage is λ phage[46]**.** A schematic representation of the lysogenic cycle is presented in Figure 6.

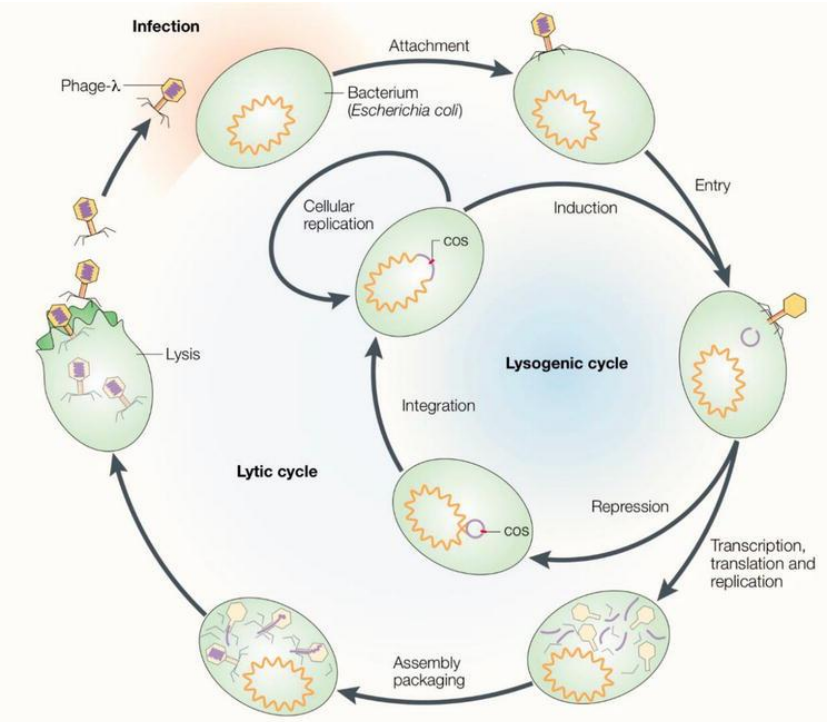

Figure 6 - Schematic representation of the lytic and lysogenic pathway. Adapted from Campbell[47].

One fundamental mechanism in replication cycle of bacteriophage is the correct host cell recognition. This mechanism is also necessary for the application of bacteriophages in capture and/or detection of bacteria, which will be explored further. This specific recognition takes place between the phage's RBPs, that are located at the tip of the tail, and a receptor located on the surface of the host cell. This specificity is directly related to the structure of receptors located on the host's cell surface. RBPs are also responsible for the correct orientation of the phage on the host cell, occurring prior to a successful infection. However, the RBPs present in the phages are different between the types of bacteria. Gram-positive bacteria are recognized through membrane components, such as peptidoglycan, teichoic acids and extracellular polysaccharides. On the other hand, gram-negative use as bacteriophage receptors cell membrane components, such as structural and transmembrane proteins (such as OmpA and OmpC), oligosaccharides and lipopolysaccharides (LPS). Other structural components from the bacterial cells can be used as receptors, such as receptors located in capsular polysaccharides (Vi-antigen), pili and flagella[48,49]. The adsorption process normally consists in three main steps: initial contact, reversible binding and irreversible attachment[50]. The first contact between the phage and the bacteria is characterized by several random phage-cell collisions caused by Brownian motion, diffusion or flow[45,50]. The following step is the reversible binding to the host receptor, but as the name suggests, it's not definitive and it's based on electrostatic forces[45,50]. This step facilitates the attachment of the phage to the cell, keeping the phage close to the cell surface as it searches for a specific host receptor[50]. When the specific receptor is found, it follows the irreversible bounding between bacteriophage and bacterial host. However, the adsorption process can differ from phage to phage. More than one receptor can be involved in the adsorption process and, in some scenarios, the phage proteins and host receptors involved in reversible adsorption are not always the same as those involved in irreversible binding[50]. An example of these type of case is the T4 phage, where the long tail fibers are responsible for the reversible binding onto LPS present in *E. coli* membrane, while for irreversible binding the short fibers interact with the heptose moiety of the host's LPS[51]. However, in the case of a T5 phage, irreversible binding is accomplished when the phage's tail protein pb5 binds with the outer membrane protein receptor FhuA, while the binding of the L-shaped fibers to the O-antigen's polymannose moiety of the host's lipopolysaccharide (LPS) of *E. coli* results in reversible binding[52,53]. Another relevant property of lytic phages that need to be considered for biosensing application is the infection time. The incorporation of lytic phages in biosensing systems can be a limitation for the detection of living cells, existing the risk of the phage lysing the bacteria before their detection it is possible. So, of extreme importance to take into account the infection time of the bacteriophage. As briefly mentioned previously, the lysis time is correlated to the absorption rate, being shorter at higher rates. The higher the concentration of bacteriophages and bacterial cells, the higher the number of collisions between these two biological elements and, consequently, the higher the adsorption rate. The rate of adsorption can also be influenced by the host physiological state and culture conditions, as well as multiple non-specific physical-chemical factors (e.g. pH, temperature, the presence of certain components and ions in the culture media)[54]. Fernandes *et. al.* studied the influence of the phage inoculating conditions, such as ionic strength and buffer pH, with the objective of avoiding the lysing of *Salmonella* cells within the time frame of the detection assay performed[55]. The authors observed a delay

in the period for cell infection and consequent bust, associating the longer lysing time to the phage not being present in ideal infection conditions. This discovery opens way to the incorporation of lytic phages in sensing applications, without the interference of the phage lytic system busting the bacterial cells before the possibility of detection. Another possible solution for this problem is the incorporation of "ghost phages", which are characterized by not having phage DNA in the interior of the capsid, in sensing assays since the lysis of the cells in dependant on the injection of the phage nucleic acids through the cell membrane. Diverse production methods for ghost phages have been reported, such as osmotic shock and alkaline treatment, both reported by Liu *et. al*[56,57]. However, the capture and detection capacity of these non-lytic phages has yet to be reported.

2.1.3.5. Bacteriophage Applications against Pathogenic Bacteria

Bacteriophages, since their discovery, are seen as potential tools against bacteria due to their unique characteristics. In the early years after their discovery, their main application was mostly focused on virology and fundamental molecular and genetic research, resulting in major breakthroughs in viral and molecular biology[33]. Currently, the application of bacteriophage properties has been a target of search in a wide range of areas, such as agriculture, biology, biotechnology, health, food safety, veterinary, pollution remediation and wastewater treatment[45]. The many advantages presented by bacteriophages make them excellent tools for various purposes, such as drug designing, delivery of protein and DNA vaccines, synthesis of novel proteins and screening of protein libraries, peptides or even antibodies. Nowadays, one of the most popular use for bacteriophages is phage display, where the phage genome is modified with the finality of displaying a desired protein or peptide on the phage surface. Lytic phages, due to their capacity to lyse bacterial host cells, are even proposed as a substitute for antibiotics, since there's been an increase of many antibiotic-resistant bacterial strains. Phage therapy as already been used in a pre-antibiotic era, proving its efficiency in combating bacterial infections and, in the present years, has been gaining popularity again. However, another emerging application of bacteriophages is as a biorecognition elements for the detection and identification of bacteria.

2.2. Magnetic Labelling of Bacteriophages for Bacterial Detection

The labelling of biorecognition elements combines the sensitivity and specificity provided by the biological molecule capable of biorecognition with the detection properties provided by the labelling agent. There is a wide range of labelling choices that can be used in biorecognition elements, such as fluorescent molecules, enzymes, radioactive isotopes, electrochemically active species, micro- and nanomaterials. However, the incorporation of nanomaterials, especially magnetic nanoparticles (MNPs), in biorecognition elements have been gaining ground in various fields during the last decade due to their unique and attractive properties.

2.2.1. Magnetic Nanoparticles

Nanoparticles are described as particles with all three dimensions in the size range from approximately 1 nm to 100 nm, possessing novel properties that non-nanoparticle based from the same materials do not have, and usually containing from hundreds to 10^5 atoms[58,59]. MNPs, which are nanoparticles that are capable of responding to an applied magnetic field, have been gaining popularity in biological and medical areas, being applied in biomagnetic concentration and separation, drug delivery, magnetic resonance imaging, and hyperthermia. These molecules come in a wide variety, differentiating in the type of core magnetic material, type of coating, size and shape, and being commercialized in many variations of said properties[60]. Regarding their size, magnetic particles have a controllable size that can vary from a few nanometers to several micrometers[60,61]. This places their dimensions to sizes comparable (or even smaller) to the sizes of biological entities, such as the previously mentioned biorecognition elements, allowing the interaction or even binding of these entities to the MNPs and the consequent tagging of those particles. However, the type of interaction between the particle and the biological elements is also dependant on the size of the MNPs compared to the later elements (Figure 7).

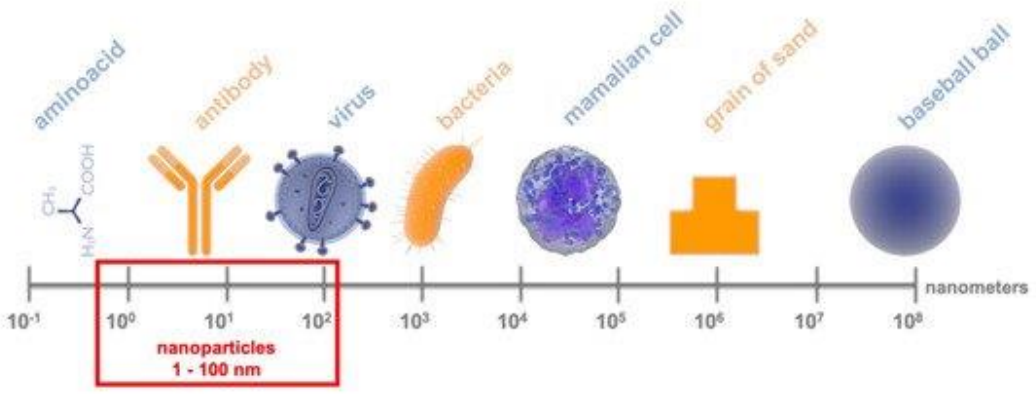

Figure 7 - Schematic comparison of nanoparticles size to other elements. Adapted from Steckiewicz *et al*.[62]

When smaller than the biological entity, the particles can either be internalized or even incorporated on the structure of the biological element. An example of this type of application is demonstrated by Liu *et. al*, where cobalt particles of about 42nm were grown on the inside of an empty T7 phage capsid (~55nm of diameter)[57]. On the contrary, when the biological element is smaller than the particles, they can be incorporated on the surface of the latter. Nanoparticles confer an additional advantage since they are characterized by having a high surface-area-to-volume when compared with microparticles or other bulk materials, offering a wider contact area. This property allows the increase of the maximum number and binding efficiency of this biological elements. In the case of biorecognition molecules, it results in lower limits of detection (LOD), being highly beneficial for detection assays[58,63,64]. The incorporation of the biological elements on the surface of the MNPs is mainly accomplished by surface modification. The main methods for the immobilization of the biological elements into the surface of nanoparticles consists of physical adsorption and covalent binding[65]. Physical immobilization is the simplest and fastest method used for the functionalization of nanoparticles, being based on the spontaneous absorption of the biological particles into the surface of the nanoparticles. However, this method provides weak interactions – van der Waals forces, electrostatic interactions and hydrogen bonds – between the two elements and the binding stability is very susceptible to external conditions (e.g. pH, temperature, ionic strength), being also dependant on high concentrations of the biomolecules to be labelled. Another disadvantage is that the non-specific adsorption of the biomolecules, resulting in random orientation and consequently affecting their properties[65,66]. Covalent binding is another alternative method of immobilization, using reactive groups present on the surface of the nanoparticle for the binding. It provides bonds of higher strength and, consequently, a more stable immobilization. However, it can also lead to loss of function or activity of the immobilized molecule due to the strong attachment. An example of this type of application can be found in the work published by Jin and colleagues, where three different aminoacids (Arginine, Lysine and poly-L-lysine) (aminoacids size can vary from 0.4 to 1 nm) were separately covalently conjugated into the surface of magnetic nanoparticles (~10nm of diameter) for bacterial detection[67].
Another relevant characteristic of MNPs is their magnetic properties. As the materials that compose MNPs are able to respond to an external magnetic field, they are also classified according to their magnetic response to the external magnetic field. This classification can be divided into three main types according to such response: diamagnetic, paramagnetic and ferromagnetic[59]. The type of response of each type of materials to an external magnetic field is schematized in Figure 8.

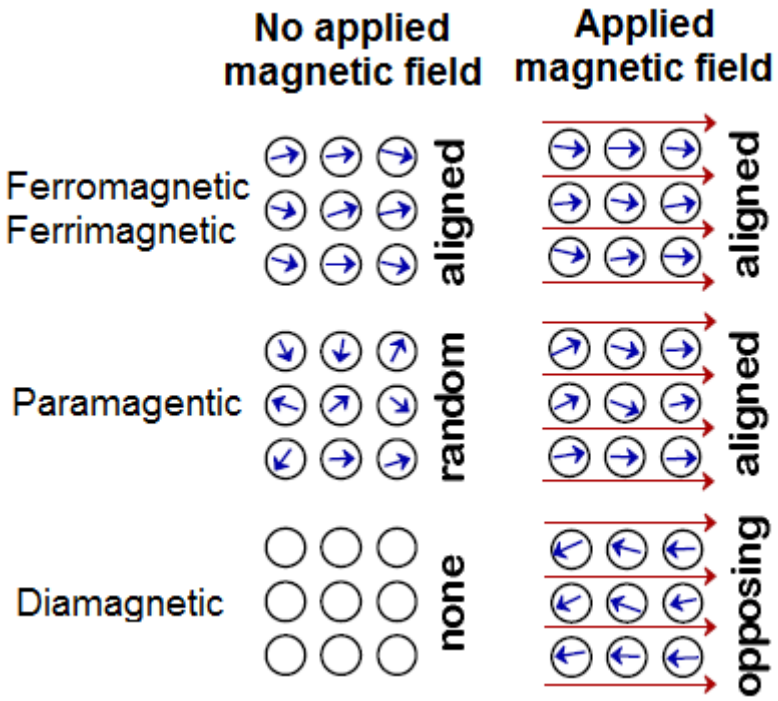

Figure 8 - Schematic of the responses of different types of materials to an applied magnetic field. Adapted from Sinatra et al.[68]

These particles can be synthesized by different chemical and physical methods, where the materials that compose the more commonly used MNPs for biomedical and biological applications commonly made of iron and iron-oxide (ferrite, magnetite and maghemite). These materials have ferromagnetic properties, meaning that, opposite to paramagnetic and diamagnetic materials, they have a large net magnetic moment due to possessing atoms with unpaired electrons. This type of materials normally have a crystal structure, where each domain has atomic magnetic moments that are parallel to each other and equal in magnitude, allowing direct coupling interactions between the moments of adjacent domains and conferring the possibility of spontaneous magnetization without the need of an external magnetic field. However, when in the presence of one, the magnetic moments of each domain align themselves along with the external field, promoting a large net magnetic moment. When the external magnetic field is removed, a residual magnetic moment persists - hysterisis[59,69]. There are many factors that can influence the magnetic properties of magnetic materials, being size one of them. In large particles (above 1 µm) there are many magnetic domains, leading to the obtention of a narrow hysteresis loop. However, in smaller particles (below 20 nm) is more probable the existence of only one domain with a net magnetic moment, resulting in a broader hysteresis loop. So, when ferromagnetic materials are divided into small particles, with a diameter small enough to present a single domain with a non-zero net magnetic moment, when submitted to the action of temperature, their magnetization direction can randomly flip. The time between the two flips is named the Néel relaxation time. When in the absence of an external magnetic field, if the time used to measure the magnetization of the particles is superior to the Néel time, their average magnetization appears to be zero. This means that there's no residual magnetism in the particle after the removal of the applied external magnetic field. In this type of situation, the particles are said to be in a superparamagnetic state. These properties represent a

major advantage in the biological and biomedical field since it prevents the aggregation of the particles (which is a problem of ferromagnetic nanoparticles)[70]. Even though they are very similar to paramagnetic particles, in the way that an external magnetic field is also able to magnetize the superparamagnetic particles, their magnetic susceptibility is much larger than the one presented by paramagnets, reacting strongly to external magnetic fields. Superparamagnetic properties can lead to the interaction between several particles due to the influence of magnetic interparticle interactions, acting as a bigger particle[71–73]. All these properties make MNPs a very powerful tool in biosensing, especially when conjugated with biorecognition elements, increasing the interest of using this type of particles as labels for molecular sensing.

2.2.2. Magnetic Labelling Strategies

One of the main advantage of magnetic biosensing lies on the absence of magnetic background coming from biological samples, which allows the magnetic labelling of biological targets with no interference that is often encountered with other reporter systems (e.g. fluorescence, electrochemistry or colorimetric-based)[74,75]. However, the labelling specificity of MNPs is conferred by the conjugation of the particles with biorecognition molecules, such as antibodies (the most popular option), aptamers and bacteriophages. The incorporation of these particles in biorecognition elements provides the benefit of incorporating both the labelling properties conferred by the MNPs and capture/detection capacity of the biorecognition elements in one single entity. Conjugation methods go from physical adsorption to covalent binding, methods that were seen more in depth previously in section 2.2.1 and allow for the incorporation of this functionalized MNPs in different assay configurations.

2.2.2.1. Clustering Assay

Clustering assays are characterized by the simultaneous binding of functionalized MNPs to a single biological target, resulting in the aggregation of the particles, as illustrated in Figure 9, resulting in a change of the T2 relaxation values of the surrounding water molecules. This change on the size of the magnetic clusters can be detected by NMR relaxometry, that detects the change in the T2 values, or Brownian relaxation measurements, that detects the change in particles hydrodynamic size[75,76].

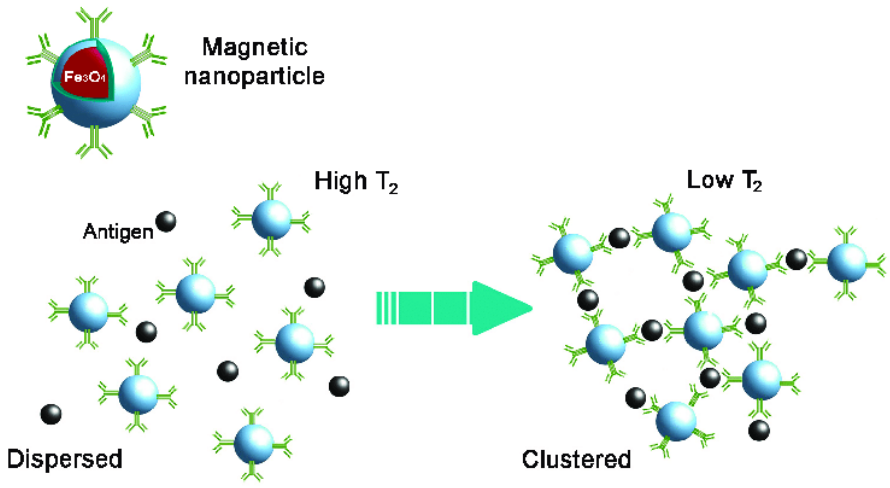

Figure 9 - Schematic representation of a clustering assay between functionalized MNPs with antibodies and their target antigens. Adapted from Shevtsov et al.[76]

This labelling method has advantages, such as the reaction taking place in the whole sample volume, allowing for faster binding kinetics than surface-based detection, and not needing washing steps to remove unbound MNPs. However, it also has disadvantages, like the need for extensive optimization for maximizing the detection sensitivity due to this method relying on the quantitative ratio between the functionalized MNPs and the biological targets[65].

2.2.2.2. Direct Magnetic Labelling

Assays that are based on direct magnetic labelling are most used for larger biological molecules, such as mammalian cells and bacteria. Due to the discrepancy in sizes, observed in Figure 5 and previously mentioned more in depth, the clustering of the functionalized MNPs is almost impossible and the immobilization of this cells on a surface is not manageable. So, it is more accessible to label directly these biological targets[65]. This type of method can consist of a one-step procedure, where the MNPs are functionalized with biorecognition molecules and directly label the cells. Another method is a two-step procedure, where first the cells are captured with the non-magnetic biorecognition element and then it is proceeded to the binding of the MNPs. The binding of these two elements is mainly achieved by the incorporation of reactive molecules on the surface of both the biorecognition molecule and on the surface of the MNPs. One of the most used interaction is the streptavidin-biotin interaction.

2.2.2.3. Sandwich Magnetic Labelling

Sandwich magnetic labelling is a more indirect method that is based on the principle of sandwich used in ELISA immunoassays, where one biorecognition molecule for the target analyte is immobilized on the sensor surface (e.g. antibodies, bacteriophages) and, after capturing the target molecule, a secondary biorecognition molecule labelled with the MNPs is added and targets the analyte, forming a "sandwich"[77]. A schematic representation of this type of labelling can be seen in Figure 10. The bound functionalized MNPs can be detected by a variety of sensors: magnetoresistant sensors, microcoils and Hall elements[65].

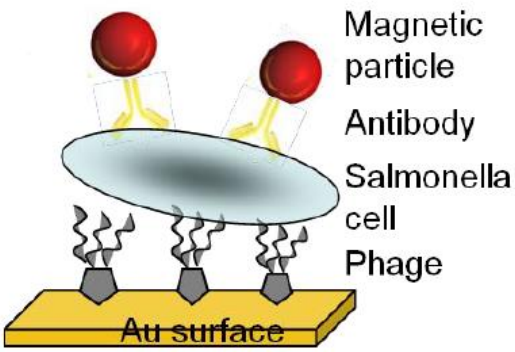

Figure 10 - Schematic representation of the "sandwich" phage-based biosensing system. Adapted from Fernandes et al[55].

2.2.3. Application of functionalized MNPS:

2.2.3.1. Magnetic Separation and Concentration:

Functionalized MNPs present the advantage of being easily manipulated through the application of an external magnetic field, allowing the separation of biological samples from complex matrixes without the need of additional sample processing (e.g. centrifugation or filtration). This method has been widely used in the capture and separation of proteins, DNA, bacteria, viruses and other biological components present in complex solutions. An additional advantage worth mentioning is that this type of separation overcomes the limitation of damaging the biological samples (such as the case of more traditional methods, e.g. centrifugation) and allows the retention of their biological activity[78]. This type of application can be mainly seen in ImmunoMagnetic Separation (IMS), where the MNPs surface is functionalized with antibodies and used as label for the target (e.g. bacteria), allowing their capture through the application of an external magnetic field and the removal of the sample background[74]. An example of this application is reported in 2009, where Pappert *et. al* used the conversion of a functional group present on the surface of the particle to an electrophilic group to conjugate antibodies to magnetic nanoparticles for the identification of enterobacterial common antigen (ECA) for the implementation in an IMS assay for *E.coli*[79]. However, this separation method can also take use of other biorecognition elements, such as bacteriophages, as to be seen later on this review.

2.2.3.2. Biosensors:

In the past decades, there was a great evolution in biosensor search for the detection and diagnosis of bacterial presence in diverse fields. When compared to the other detection methods more commonly used for the detection of bacteria, biosensors demonstrated to be great substitutes, mainly due to their excellent performance - low cost, fast response, high sensitivity, and high selectivity[80]. A biosensor is usually composed by an analyte (a target that will be sensed), a biological recognition element (bio-probe/bio-receptor), a transducer and an electronic system that will amplify, process and display the signal. When the biological recognition material recognizes the analyte, it will interact with it, generating a catalytic or binding event. Then, detectable signals, that are proportional to the analyte

concentration, are produced and captured by the transducer. Then the output from the transducer is then amplified, processed and saved as a measurable effect (Figure 11)[6,80].

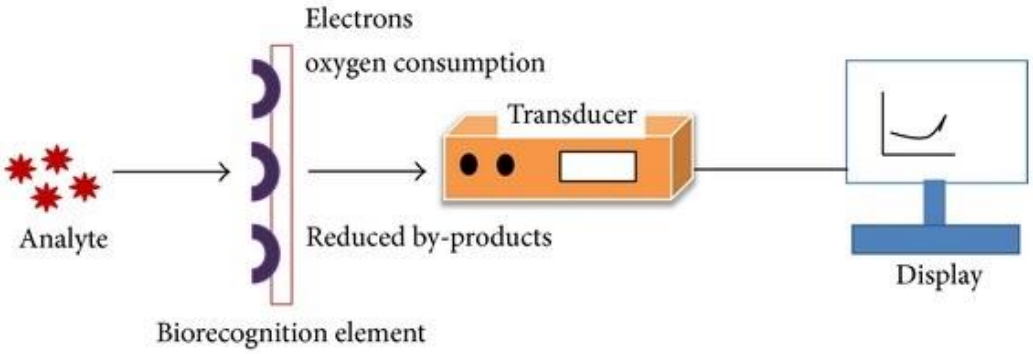

Figure 11 - Schematic representation of a biosensor functionalization. Adapted from Dhull et al[81].

Biosensors can be classified either by their biomolecular elements (e.g. antibodies, enzymes) or by their transducer principle. A classification of biosensors by their incorporated transducer is represented in Figure 12.

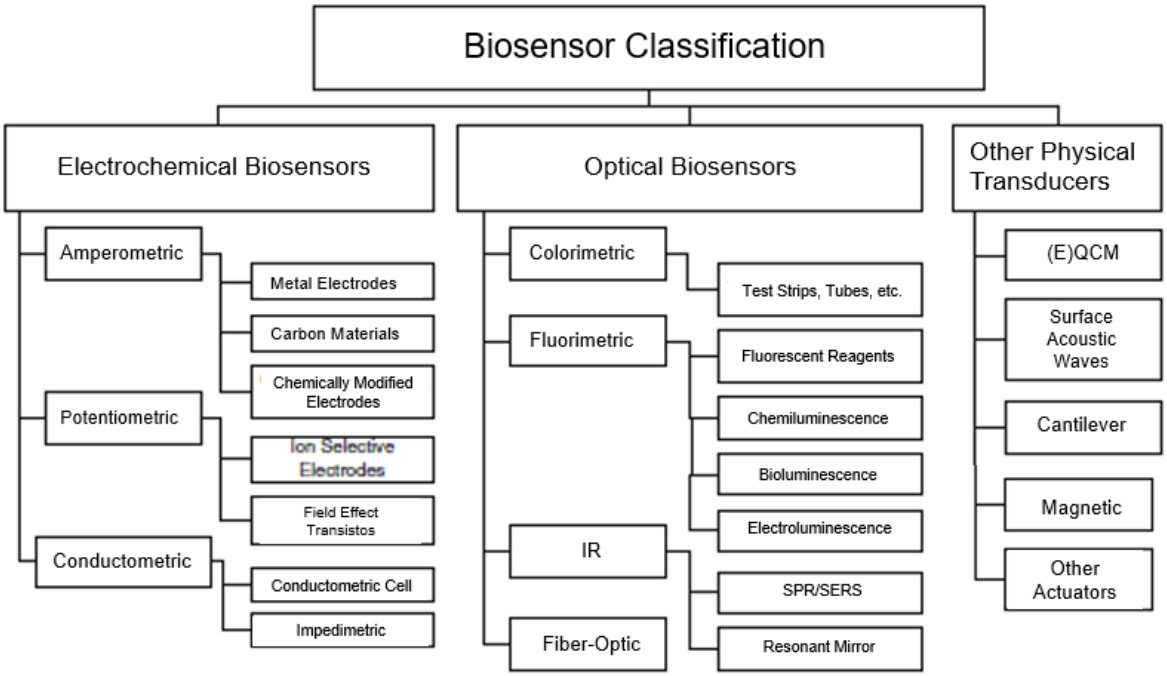

Figure 12 - Schematic representation of the classification of biosensors in accordance with the transducer/signal transduction principles. Adapted from Gennady Evtugyn[82].

The signal detection in biosensors can also be improved by the incorporation of conjugated particles, including magnetic nanoparticles. MNPs have also been reported as a way to improve the efficiency of biosensors, either by biological labelling the samples or by amplifying the signal, having increased the attention on MNPs based biosensors. Magneto-based biosensors offer many advantages

over the conventional sensing methods, such as the small size, low cost, high sensitivity, biocompatibility and low power[83]. The most relevant type of magnetic-based biosensors for the developing project are magnetoresistive biosensors.

2.2.3.2.1. Magnetoresistive biosensors:

Magnetoresistive biosensors have been considered as promising candidates for the detection of MNPs, being used to detect biomolecules from DNA and proteins to bacteria. They are based on the change of resistance under the influence of an external magnetic field[84]. Magnetoresistive sensors can be used to detect the presence of MPs by the change on their electric resistance by the fringe field of the MPs, resulting in detectable electrical current changes within the sensor. A typical transfer curve found in magnetoresistive sensors is represented in Figure 13, representing the behaviour of this type of sensor with the strength of the magnetic field applied. This type of graphic representation can give information regarding the MR ratio, which represents the change of resistance that occurs when the magnetic field changes from one direction to the other, and the sensitivity of the magnetic sensor, given by the slope of the transfer curve at a certain magnetic field strength[84].

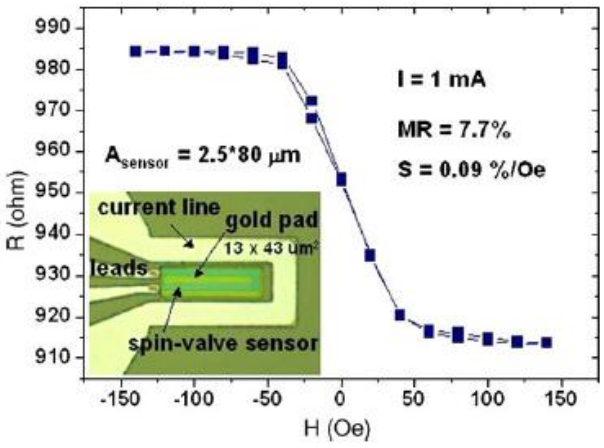

Figure 13 – Transfer curve for magnetoresistive sensors. Adapted from Martins *et. al*[85].

The GMR was discovered in 1988 by the team of Albert Fert (Baibich 1988) in France on Fe/Cr(001) multilayers and, independently, by Peter Grünberg (Binash 1989) and coworkers in Germany on Fe/Cr/Fe(001) trilayers, which won the 2007 Nobel Prize in Physics for this discovery[86,87]. The authors discovered a large resistance decrease, up to 50%, when applying an external magnetic field in a sandwich-type composed by a ferromagnetic and a paramagnetic compound (Fe and Cr). When the multi-layer structure composed by alternating magnetic thin films and non-magnetic spacers is not in the presence of an external magnetic field, the magnetic spins of the ferromagnetic material is coupled in an anti-parallel direction of their neighbouring ferromagnetic layer, resulting in spin collision at the interfaces between the ferromagnetic and non-magnetic layers, being in a high resistance state. However, when exposing the materials to an external magnetic field, the ferromagnetic layers magnetization is saturated in the field's direction, resulting in a parallel alignment of the magnetic spins. This results in not existing spins collision at the interfaces of the magnetic and non-magnetic layers, resulting in a low resistance state[88].

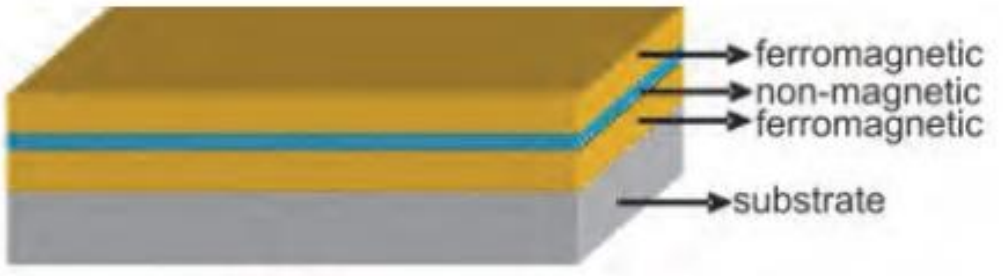

Figure 14 - Schematic representation of a GMR multi-layered sensor. Adapted from Ramli *et al*[89].

GMR sensors have been mainly applied in computer storing technology however, in the last decade, biosensors based on GMR have been gaining popularity due to their potential as sensing elements for biomolecular detection[89,90]. In 1998, Baselt *et. al* developed a GMR based biosensor, the Bead Array Counter (BARC). This sensor detected magnetic fields produced by paramagnetic particles immobilized directly above the surface of the sensor during antibody–antigen binding assays, being the first system to sense biomolecular labelled MNPs[91]. This showed the potential in the development of GMR sensors for biomolecule detection, increasing the research in this type of biosensors. One example of the application of GMR based biosensors is reported by Li *et. al*, where a GMR system was developed with the objective of the detection, in unprocessed human sera, of interleukin-6 (IL-6)[92]. Two methodologies where tested. First, the sensor surface was functionalized with capture antibodies, which will capture the IL-6 biomarker. Then, a sandwich between the antigen and magnetically labelled antibodies will be formed (Figure 15.A). In the second methodology, instead of using magnetically labelled antibodies, the authors captured directly the magnetically labelled analyte on the GMR biosensor (Figure 15.B). In both methods, the detection of the magnetic signal was made through the creation of a dipole field by the particles captured (Figure 15.C), demonstrating the GMR sensor sensitivity to distance. The presented properties of this type of sensor demonstrated potential for lab-on-a-chip applications, eventually leading to the production of a low-cost point-of-care (POC) device.

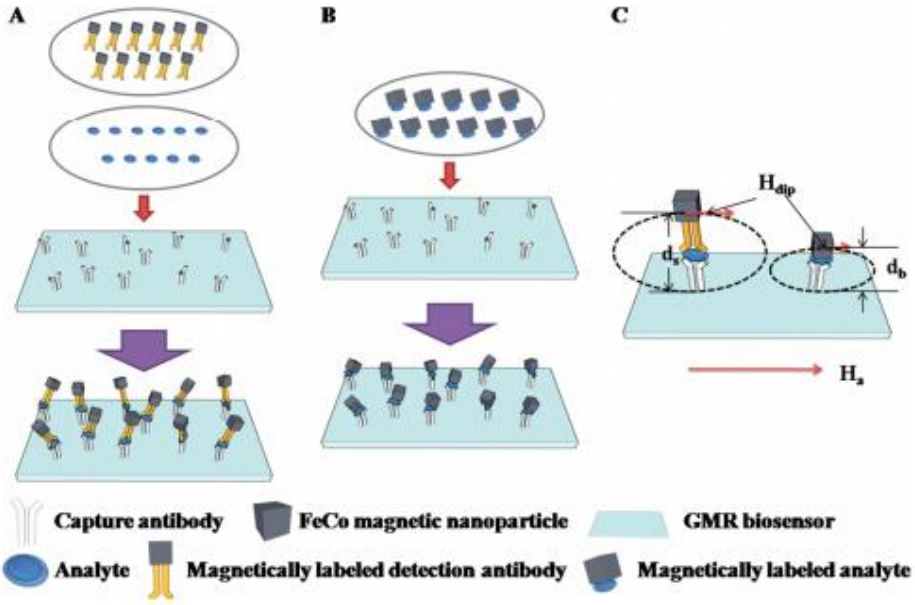

Figure 15 - Schematic representation of the two GMR based biosensors developed by Li et. al. **A-** GMR sensor based of a sandwich labelling approach. The sensor surface is first functionalized with antibodies, followed by the labelling of the bound analyte with secondary MNP-labelled antibodies. **B-** GMR sensor based of a direct labelling approach. The sensor surface is first functionalized with antibodies, followed by the direct labelling of the bound analyte. **C-** GMR biosensor working principle. Adapted from Li et. al[92].

Spin-valve biosensors are a particular type of GMR sensors that are largely used in biomolecular recognition detection[85,93,94]. These sensors are normally composed by three different layers: a non-magnetic layer sandwiched between two ferromagnetic layers, one of which is pinned by an antiferromagnet and its magnetization does not change with the external field, while the other is a free layer that will act as a switch of the spin-valve rotating with the external magnetic field. When magnetic layers have parallel magnetization directions, the spin-up electrons will be weakly scattered, while the spin down electrons will be strongly scattered. This will lead to a low resistance state, However, when the two magnetic layers magnetization is in an antiparallel direction, the electron spins will be both strongly and weakly scattered, no matter the spin direction. This creates a high resistance state[95,96].

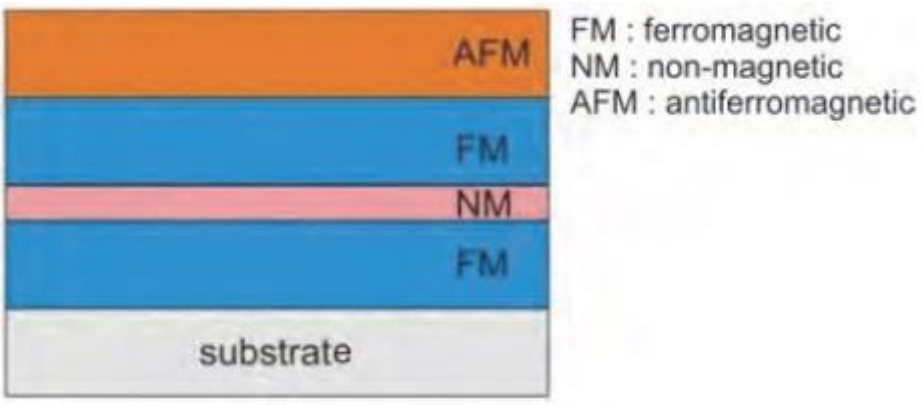

Figure 16 - Schematic representation of a GMR spin-valve sensor. Adapted from Ramli et al[89].

One example of application is the biosensor developed in Fernandes *et al*, where a "sandwich"-type of biosensing system for bacteria incorporating bacteriophages as capture elements and MNP-labelled antibodies as labelling and biorecognizing elements (Figure 10) was developed[55]. The used sensor is composed by two distinct sensing areas arranged in two columns, each being composed by 3 groups of 5 spin-valve sensors. One sensor is used as reference, while the probe sensors on the biochip terminate with exposed Cr/Au pads with magnetoresistive sensors underneath, which will detect the magnetic nanoparticles. The quantitative detection and distinction between viable to non-viable cells was possible, demonstrating a high sensitivity.

The TMR effect is based on the spin-dependent tunneling of a quantum mechanical effect, between two ferromagnetic layers are separated by a thin insulating layer, allowing electrons to tunnel across the non-conductive barrier[90]. This insulating barrier is normally composed by Al_2O_3, MgO, Ga_2O_3, MgO or graphene, while the ferromagnetic layer is composed by a conducting material, like cooper[90,95]. TMR sensors are also known as magnetic tunnel junctions (MTJ) sensors. When compared to the previously mentioned sensors, MTJ presents a highest MR, being reported MR as high as 220% at room temperature and 300% at low temperatures when using a tunnel barrier composed by MgO[97]. TMR biosensors have also been produced to detect MNPs at low concentrations, as reported by Shen *et. al*., opening opportunities for the quantitative detection of MNP-labelled biomolecules[98,99]. TMR sensors have already been used to detect DNA, protein and even bacteria. Wu *et. al* developed a TMR sensor for the detection of *E. coli* O157:H7[100]. The capture of the bacteria done using a magnetic immunoassay, where antibodies were immobilized at the surface of the biosensor. The labelling step is based on sandwich-labelling, where MNP-labelled antibodies bind to the captured cells. These magnetic probes then induced a weak magnetic signal, which was detected by the TMR sensor. A detection limit of 100 CFU/mL *E. coli* O157:H7 bacteria in 5 hours was reported by the authors, showing a promising application in rapid food safety and biomedical detection. These results open's way for the adaptation of this type of sensors to the use of other magnetically labelled biorecognition molecules, reducing their production cost.

2.2.4. Labelling of Bacteriophages as a Tool for Bacterial Detection

As briefly mentioned previously, the use of magnetic nanoparticles as label for biorecognition molecules present many advantages, such as: (1) allowing the labelling of the recognition agent and, consequently, the target molecule; (2) increasing the potential of manipulation of the target molecules through capture; (3) target cell concentration; (4) magnetic detection. As mentioned previously, MNPs have a large surface-area-to-volume, providing benefits for the binding of biological molecules to their surface, increasing the capture and detection potential of both the magnetic materials and the biologic entity. This type of applications has used, in their majority, the conjugation with biological recognition elements, such as antibodies, as seen previously, being especially popular in IMS. This type of magnetic separation is one of the most conventional methods, being the main steps the incubation of the bioconjugates with target, consequently magnetizing the bacteria through its labelling, and the capture of it through the application of an external magnetic field. The sample background can be removed and

the magnetic particles ressuspended in a smaller volume of buffer solution[74]. However, these types of methods can also be translated for bacteriophages, which present an attractive alternative to other recognition elements, allowing the overcoming of some drawbacks associated to magnetic separation with other biorecognition elements (e.g. the identification of false positives due to non-specific interactions with non-target cells and the magnetic biorecognition element). The first bacteriophages conjugated with nanoparticles able to isolate and capture bacteria were reported in 1997 and 2001, by Janczuk *et. al* and Chen *et. al* respectively. However, the capture efficiency obtained in both studies was very low, presenting values under 20%[101,102]. Several years after, Liebana *et. al* attempted to incorporate the conjugation of nanoparticles with bacteriophages for bacterial separation[103]. They immobilized a P22 bacteriophage on tosylated magnetic particles, resulting in the capture and concentration *Salmonella* (host bacteria) cells through phagomagnetic separation without the need for filtration or centrifugation. In this article, the bacterial separation was followed by bacterial detection by electrochemical magneto-genosensing, resulting in detection values as low as 3 CFU/mL in 4 hours, presenting a huge improvement when compared to the previously mentioned articles. However, the detection procedure required expensive reagents and equipment and englobed a multi-step procedure, not being ideal for commercialization against other similar procedures. In 2015, Chen and colleagues developed nanoscale bacteriophage-tagged magnetic probes for *E. coli* cells capture and separation, inspired by methodologies that use antibody-tagged magnetic particles for analyte capture from liquid samples[104]. In this report, T7 bacteriophages were bound to magnetic nanoparticles**.** The nanoparticles were coated with a silica shell, where streptavidin was immobilized for subsequent conjugation of biotinylated T7 bacteriophage and antibodies for comparison**.** The magnetic probes were incubated with the bacteria, 30 minutes for the conjugated antibodies and 15 minutes for the conjugated bacteriophages. This difference in incubation time between biological elements is mainly to avoid the risk of the bacteriophages lysing the bacteria and affecting the efficiency of the procedure. Even though the bacterial capture efficiency was not significantly different between the bacteriophage magnetic nanoparticles from antibody magnetic nanoparticles**,** bacteriophages still present more advantages over antibodies (cost of production, robustness, resistance to extreme conditions, distinction over viable from non-viable cells). Overall, bacteriophages conjugated with magnetic nanoparticles still presents as an improved separation/concentration tool. In the same year, the same group of researchers developed a bacteriophage-based biomagnetic separation method for the detection of *E.coli*, using the same type of of conjugation for the bacteriophages and the particles as in the previous study. In this article, the authors archived the capture of 86.2% *E.coli* cells present in broth within 20 minutes and, the detection protocol with an additional PCR step resulted in detection limit of 10^2 CFU/mL in less than 3 hours. Recently, a novel method for bacterial detection and separation was developed. In 2017, Janczuk *et al.* conjugated T4 bacteriophages, specific for *E.coli*, with bifunctional magnetic-fluorescent submicroparticles through covalent binding and used flow cytometry as a detection method[105]. The measured capture efficiency of the labelled phages varied from 10 to 10^5 CFU/mL while the magnetic separation coupled with flow cytometry provided a detection limit of 10^4 CFU/mL. While the authors provided an easy and fast detection assay, the detection limit is still quite high when compared to other assays. In 2006, Liu *et. al* developed a new type of magnetic biorecognition probe. The authors used

the growth of metallic Co particles on the inside of a “ghost phage” capsid – phages without DNA – to magnetize the biomolecules. However, the capture/detection capacity of this new magnetic nanoprobes was not tested. Nevertheless, this opens way for the investigation of new conjugation methods that could tackle problems associated to the normally used conjugation processes.

3. Thesis Proposal

The use of magnetic nanoparticles as label for biorecognition molecules present many advantages, being mentioned in the previous section. However, one of the main obstacles encountered in the conjugation of biological molecules in the surface of magnetic nanoparticles, or even the possible conjugation of the particles on the external part of the bacteriophage, is the possibility of affecting specific biorecognition events based on surface receptors. The main cause is that the main mechanism for bioconjugation for bacteriophages is through affinity binding or cross-linking. Since the conjugation mechanism is uncontrollable, it can lead to the anchoring of the biomolecule in a domain responsible for the recognition event. Additionally, it can also lead to the lysis of the target bacteria before their detection. With these adversities in mind, this project aims to develop a novel magnetic-based nanoligand through the incorporation of the magnetic nanoparticles inside the bacteriophage capsid. Such type of magnetic probe would have the benefit of having the magnetic labelling capacity and biorecognition mechanism in only one biomolecular entity that brings advantages when compared to other biorecognition molecules, e.g. antibodies. Such type of magnetic nanoprobe could be incorporated in both dynamic and static detection systems for bacteria. In case of success, the methodologies incorporated for the production of the magnetic bacteriophages could also be further optimized and translated into antibody titration, through the magnetization of viral particles. Such conjugation to be studied in this project has as a base the destabilization of the phage protein capture, being hypothesized the creation of gaps in the protein capsid that are wide enough to allow the internalization of MNPs. The first step of this project starts with the phage conjugation with magnetic nanoparticles under different conditions, followed by the characterization of phage conjugates exploring Transmission Electronic Microscopy (TEM) technic and the further assessment of the conjugation efficiency using magnetoresistive phage based-sensors developed in INESC-MN was planned. However, some limitations surged along the thesis due to the pandemic situation, leading to a shorter time period for the experimental work. For the presented reasons, the experimental work was not fully performed as planned, especially the characterization of the magnetic bacteriophages in the biosensor.

4. Materials and Methods

4.1. Bacterial strains, bacteriophages and culture media

The bacteria and bacteriophages used in this study were: *Escherichia coli* (*E. coli*) with the corresponding bacteriophages, T4. *E. coli* bacteria and bacteriophages used were obtained from the company Dsmz (Braunschweig, Germany). The bacteria strains used in this study were grown on Tryptio-Casein Soy Broth (TSB) media at a temperature of 30-40ºC under agitation (200-300 rpm) or in solid plates containing Trypto-Casein Soy Agar (TSA). Both growth media were provided by Biokar Diagnostics (Beauvais, France).

4.2. Phage conjugation with magnetic nanoparticles:

4.2.1. Osmotic Shock:

Osmotic shock was performed as a method of conjugation for the interiorization of the permanent magnetic nanocomposite of magnetite (MNPs) into the bacteriophage's protein capsid. With this objective in mind, to study the efficiency of the method, three different conditions were tested: samples with bacteriophage only, and samples with bacteriophage with MNPs added after and before performing the osmotic shock. To the samples with MNPs, it was added approximately 10 mg of NdFeB magnetic particles (Magnequench), with an average diameter of 5 nm. Osmotic shock was performed using $C_2H_3NaO_2$ 4M as hypertonic solution and used in a proportion of 1:1, where 500 µL of phage solution was added to a sterile 50 mL falcon, along with 500 µL of hypertonic solution. The samples were left incubating on ice, where the time of incubation was varied (5, 10, 15, 20 and 30 minutes). After the time of incubation, 50 mL of autoclaved chilled water was added. The obtained samples were characterized and stored at 4ºC. After the treatment, the samples were submitted to magnetic separation. Due to the large size of the falcons, an individual magnet was used as an option instead of a dedicated magnetic concentrator. The samples were submitted to 2 minutes of magnetic separation, with the magnet placed against the falcon wall, at the bottom. The supernatant was collected, and the magnetic pellet was washed with 5 mL of SM buffer. The samples were again magnetically separated for 2 minutes, and the supernatant collected. The same procedures were repeated one additional time, obtaining a magnetic pellet at the end. All samples – supernatant, washes supernatant and magnetic pellet - were collected, stored at 4ºC till further characterized. Further into testing, the final obtained magnetic pellet was washed with 5 mL of SM buffer two additional times, according to the last described method, resulting in a magnetic pellet. All samples – washes and magnetic pellet - were collected, stored at 4ºC till further characterized.

4.2.2. Sonication:

Sonication in ultrasound bath was performed as a second method of conjugation for the study of the interiorization of the MNPs into the bacteriophage's protein capsid. The sonication treatment was applied to samples of 1 mL of phage solution and to samples of 1 mL of phage solution with 20 mg of NdFeB magnetic particles. Sonication was performed in an Ultrasonic bath USC TH (VWR, Amadora, Portugal) at 45 kHz with an initial temperature of 10ºC. Five different sonication times were tested for

each sample (15, 20, 30, 40 and 60 minutes). The obtained samples were characterized and stored at 4ºC until further testing. Afterwards, the samples were submitted to magnetic separation. For that purpose, a DynaMag™ Magnet (Invitrogen, ThermoFisher) for 2 mL samples was used. The samples were submitted to 2 minutes of magnetic separation. The supernatant was collected, and the magnetic pellet was washed with 1 mL of SM buffer. The samples were again magnetically separated for 2 minutes, and the supernatant collected. The same procedures were repeated three more times, resulting in a total of four washes and one final magnetic pellet. The supernatants and the magnetic pellet were collected. All samples were stored at 4ºC till further testing.

4.3. Phage Characterization:

4.3.1. Phage Titration:

Phage titration was used as a characterization method for the study of the conjugation of MNPs with the bacteriophages in solution. To start the procedure, a pre-inoculum of the host-bacteria correspondent to the phage be amplified was prepared in a 15 mL falcon containing 5 mL of TSB medium and grown at 30-40ºC with vigorous agitation (20-300 rpm) overnight. After approximately 18h, the overnight grown cells were re-inoculated in about 5 mL of medium at an initial optical density at 600 nm (OD_{600}) of 0.1 as measured in the Hitachi U-2000 spectrophotometer. The cells were grown at 30-40ºC with vigorous agitation (20-300 rpm) till an OD_{600} of 0.25-0.30. Meanwhile, 100 µL of phage stock was serially diluted in 900 µL of SM buffer. After reaching an OD_{600} of 0.25-0.30, 20-100 µL $MgCl_2$ (Sigma-Aldrich, St.Louis, MO, USA) was added to the inoculum. The 100 µL of each appropriate dilution was added to 100-300 µL of $MgCl_2$ containing inoculum and incubated for 15-30 minutes at 30-40ºC without agitation. Then, to each dilution it was added 2-4 mL of molten top agar (3.5 g agar-agar, 12.5g TSB powder, 500 mL Milli-Q H_2O) with $MgCl_2$ (10 µL $MgCl_2$ per 1 mL of top agar), gently mixing it and pouring into TSA plates. The plates were incubated at 37ºC without agitation overnight. The titer of the samples was calculated.

4.3.2. Bradford Protein Assay:

Bradford assay was also used as a characterization method for the study of the conjugation of MNPs with the bacteriophages in solution. A microwell plate was used, where 50 µL of each sample and the controls were pipetted into the wells. The BSA samples, with the concentrations described in Table 3, were also pipetted into the wells in the same volume. Duplicates of all samples were made. Using a multichannel pipette, 200 µL of Coomassie solution were added to each well. The plate was mixed for 30 seconds and incubated for 10 minutes at room temperature. The absorbances where measured in a Multiskan FC Microplate Photometer (Thermo Fisher) at 595nm. The samples protein concentration was obtained through the construction of a BSA standard calibration curve.

4.3.3. Transmission Electron Microscopy (TEM):

TEM was utilized with the finality of characterizing the bacteriophages and confirming if the conjugation of the particles with the phages was successful. The procedure was accomplished in MicroLab, IST (Lisbon, Portugal). Uranyless was used as a negative staining agent. The T4 phage solution and a sample with T4 phage solution with added MNPs in suspension were one time diluted for visualization, for the same reasons mentioned previously. Treated samples were used directly. The phage suspensions were dripped onto a carbon-formvar coated grid and fixed for 1 min. The liquid in excess was removed by tight contact with absorbent paper. The grid was left air-drying for 30 s at room temperature, followed by the negatively staining with UranyLess (Delta Microscopie, Mauressac, France).

5. Results and Discussion

5.1. *E. coli* phage conjugation with MNPs

5.1.1. Osmotic Shock

Osmotic shock is a technique that has been used as a chemical method for cell disruption. It is based on the water movement from inside of the cell to the outside, or the opposite, due to the sudden exposition to high or low salt concentration of the external environment. However, such method has also been used to produce phages without their encapsulated DNA – "ghost phages". According to the report of Liu *et al.*, osmotic shock was used to disrupt a T7 capsid, allowing the escape of DNA debris[56]. However, even though the disruption of the capsid proteins was sufficient to allow the escape of the T7 DNA, resulting in the successful obtainment of ghost phages, the capsid appeared to maintain its integrity, even though slightly shrunken. Based on this, osmotic shock was used as a possible conjugation method with the hypothesis that the protein capsid would be destabilized enough to enable the passage of the magnetite MNPs to its interior, while maintaining its integrity. T4 *E. coli* bacteriophage was selected to proceed the planned experimental work. Since it was already available in the lab a prepared T4 stock, it was possible to move directly into testing. Additionally, the paired *E. coli* bacteria has been previously worked with in IST-iBB, having already established growth curves for the bacteria, especially the time needed to reach an OD_{600nm} of 0.25 – 0.30. First three different types of samples (phage only, phage with MNPs added before performing osmotic shock and phage with MNPs added after osmotic shock) were submitted to 5 different times of incubation (5, 10, 15, 20 and 30 minutes) with the hypertonic solution, followed by the addition of water. After performing the treatment, an aliquot of each sample was taken and titrated.

5.1.1.1. Bacteriophages Characterization

5.1.1.1.1. Samples Titration

With the finality of characterizing the samples submitted to osmotic shock, a phage titration was performed according to the previously mentioned protocols. As controls it was used a sample containing 500 µL of T4 bacteriophage diluted in 50 mL of autoclaved water and 500 µL of T4 bacteriophage with 10 mg of the magnetic nanocomposite MNPs (provided by INESC-MN) diluted in 50 mL of autoclaved water. The phage titration method is based on the counting of plaque forming units in a bacterial lawn, assuming that each plaque unit comes from one single phage that successfully infected the bacteria present in that region. However, the plaque counts on each plate should be between 30-300 to ensure the reliability of the method. With this in mind, after incubation, plaque units were counted to obtain the number of plaque forming units per milliliter (PFU/mL) using equation 1:

$$\frac{PFU}{mL} = \frac{Number\ of\ plaques\ counted\ x\ Dilution\ factor}{Inoculum\ Volume} \quad (1)$$

The results are presented in Table 1. The number of infectious phage particles present in solution was also calculated for each sample, shown in Table 2. The (%) of infectivity loss when

compared to the initial phage concentration was also calculated, being shown in Table 8.1 in the Attachments.

Table 1- Osmotic Shock samples phage concentration in PFU/mL for each incubation time.

Incubation Time (min)	Phage Only	Phage + Particles (Before)	Phage + Particles (After)
5	4.30E+07	1.70E+08	1.13E+08
10	3.28E+08	1.81E+08	1.80E+08
15	1.52E+08	1.63E+08	0.00E+00
20	8.10E+07	1.76E+08	5.00E+07
30	6.80E+07	1.52E+08	2.00E+07

Table 2- Number of phages present in each sample after the osmotic treatment.

Incubation Time (min)	Phage Only	Phage + Particles (Before Osmotic Shock)	Phage + Particles (After Osmotic Shock)
5	2.15E+09	8.50E+09	5.65E+10
10	1.64E+10	9.05E+09	9.00E+09
15	7.60E+09	8.15E+09	0.00E+00
20	4.05E+09	8.80E+09	2.50E+09
30	3.40E+09	7.60E+09	1.00E+09

To better visualise the obtained results, the values from Table 2 were converted to a column chart, presented in Figure 17:

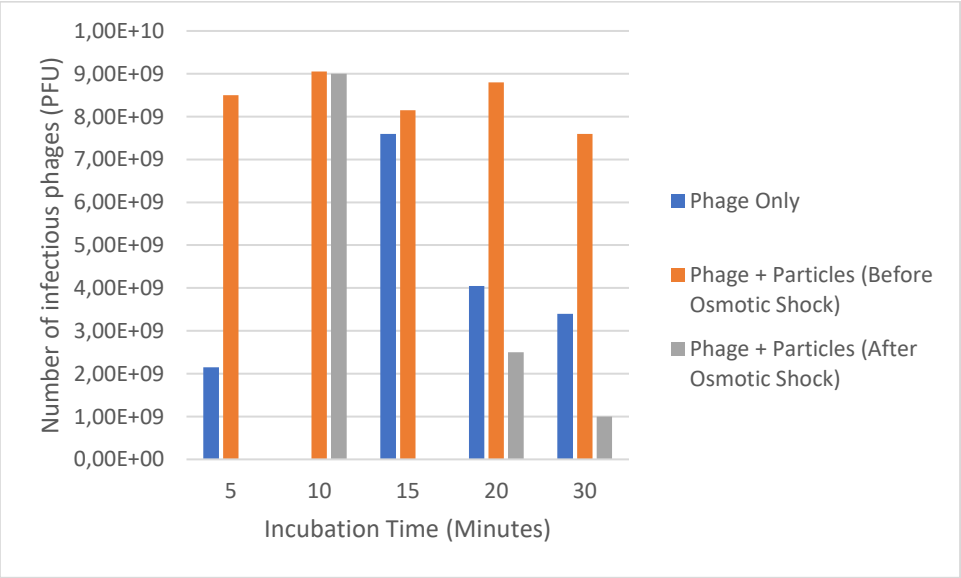

Figure 17 - Evolution of the number of T4 phages present in each sample after the osmotic treatment with the incubation time. Values from the condition Phage + Particles (After Osmotic Shock) at 5 minutes of incubation and Phage Only at 10 minutes of incubation were excluded.

The previously mentioned controls, the sample with only phage diluted and the sample with phage and MNPs diluted, were also titrated, resulting in a concentration of 2.86×10^8 PFU/mL for both samples. The number of infectious phages was also calculated for the controls, obtaining a value of 1.43×10^{10} for each control. When comparing the number of infectious phages present in samples treated with osmotic shock with the obtained in the control, an average infectivity reduction of 70% occurred. However, it is worth noting the obtained infectious phage number for 10 minutes of incubation time, where it appears that the phages did not lost infectious capacity. Additionally, it appears to have a slight increase in the number of infectious phages when compared to the control. Due to this pattern not being seen in any other sample, this result can be attributed to titration errors, not being accounted for the calculation of the average infectivity reduction. On a similar note, the samples correspondent to the addition of the MNPs after the submission of the phage particles to the osmotic shock conditions suffered an average infectivity reduction of 71% when compared to the control. However, is worth noting the obtained infectious phage number for 5 minutes of incubation time, where it appears to increase this number when compared to the control. The most probable cause for this obtained result is the occurrence of errors during the titration procedure, since this pattern was not found in any more samples. Additionally, when analysing the result obtained from the sample Phage + Particles (After) incubated for 15 minutes, it appears that it lost all infection capacity. However, when compared to the higher incubation times for the same sample, it still presents infectivity. Also, as seen in later chapters for the analysis of further testing, it appears to have infectious phages present in solution. So, the obtained result can also be attributed to titration errors and it was not accounted for the loss of infectivity. Regarding the incubation time, a similar result can be seen in both conditions (phage only and phage with particles were added after the treatment), where a gradual decrease in the number of infectious phages can be seen between 10, 20 and 30 minutes of incubation time, going to a loss of infectivity as high as 93% at an incubation time with the salt of 30 minutes for the condition Phage + Particles (After). To confirm this gradual decrease in infectivity, the titration of samples from incubation times 5 and 15 minutes should be repeated. Additionally, after some search in literature, it was found an article by Anderson *et. al* where it was reported that when submitting suspensions of T2, T4 and T6 phages to high concentrations of salt and then quickly diluting them, the phages lost infectivity capacity and “ghost” phages appeared in solution. So, is possible to assume that the decrease in the number of infectious phages observed in the samples with only phage in solution can be due to either escape of the phage DNA from the capsid, consequently producing ghost phages in solution, or to the complete busting of the phage capsid. However, when observing the samples with osmotically treated phages with MNPs added posteriorly, it was obtained the highest loss of infectivity when incubating with 30 minutes of hypertonic solution. It is possible that the same scenario happened, since the average loss of infection value is very close to the obtained in the samples with only phage. However, when observing the results for the phages treated along with the MNPs, it was obtained a smaller percentage of loss of infectivity (41%). One possible scenario is that, when submitting the phages to osmotic shock, the capsid was disrupted enough to allow the entrance of MNPs. However, these particles could have avoided somehow the release of the phage DNA from the capsid, and the phages maintained their infection capacity.

5.1.1.1.2. Bradford Protein Assay

To access the possible capsid degradation due to the applied chemical method (osmotic shock), the protein concentration of the phages in solution was measured through a Bradford Protein Assay. A standard curve was obtained using Bovine Serum Albumin (BSA), presented in Figure 18, along with the correspondent equation. The BSA concentrations and correspondent Abs_{595nm} values are represented in Table 3.

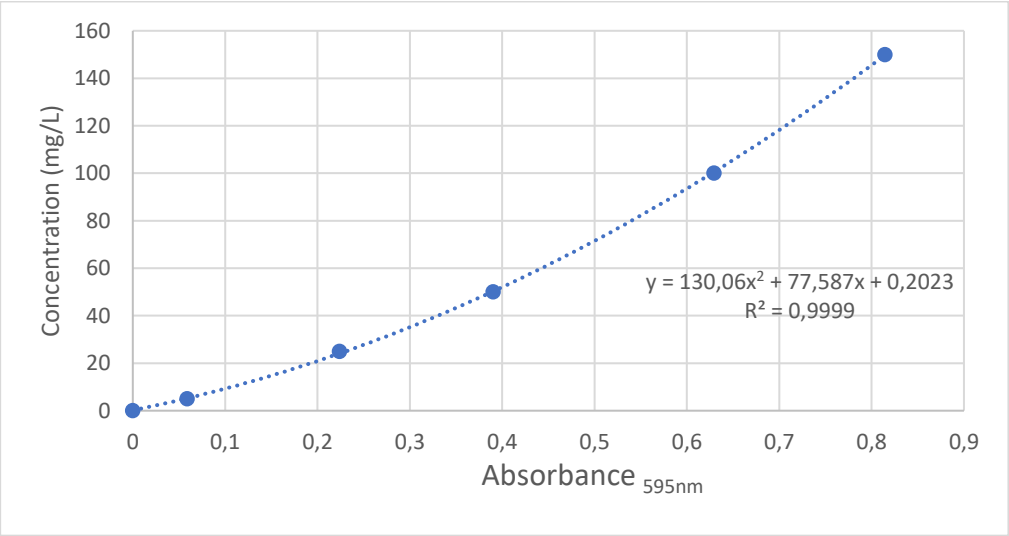

Figure 18 - Graphical representation of the standard curve obtained for BSA. The equation obtained from the linearization of the graphic is: $y= 130,06x^2 + 77,587x + 0,2023$.

Table 3 - Bradford protein assay obtained absorbances at 595nm for each BSA concentration in mg/mL.

BSA Concentration (mg/L)	Abs595nm
400	0.9433
300	0.8042
200	0.6529
150	0.5617
100	0.4555
50	0.2799
25	0.1983
5	0.0345
0	0.0000

The same controls used in the previous section were also used in the Bradford Protein Assay, with the addition of a sample with 10 mg of magnetite MNPs diluted in 50 mL of autoclaved water. The obtained results can be observed in Table 4:

Table 4 - Bradford protein assay obtained absorbances at 595nm for each sample and the correspondent conversion to protein concentration in mg/mL.

	Phage		**Phage + Particles (Before Osmotic Shock)**		**Phage + Particles (After Osmotic Shock)**	
Incubation Time (min)	Abs595nm	[Protein] mg/L	Abs595nm	[Protein] mg/L	Abs595nm	[Protein] mg/L
5	0.0142	1.326	0.0043	0.538	0.0109	1.063
10	0.0117	1.124	0.0060	0.673	0.0086	0.879
15	0.0145	1.355	0.0073	0.776	0.0093	0.935
20	0.0026	0.570	0.0006	0.562	0.0088	0.895
30	0.0122	1.168	0.0040	0.511	0.0063	0.696

As for the controls, the samples with diluted T7 phage and with T7 phage with particles reported a protein concentration of 1.2370 mg/L and 0.5620 mg/L respectively. As for the control with the particles only, it reported an absorbance at 595 nm of -0.004, which is expected since there is no protein in solution to react with Coomassie solution. In a first analysis of the results obtained from the controls, it is possible to affirm that the MNPs in solution do affect the reading of the absorbance, obtaining significant different reads from bacteriophage without and with MNPs. Additionally, when preparing the samples on the multi-well plate, a reaction between the samples containing MNPs and the Coomassie reagent took place, reported in Figure 19, producing foam that could affect the reading of the samples when in the plate reader.

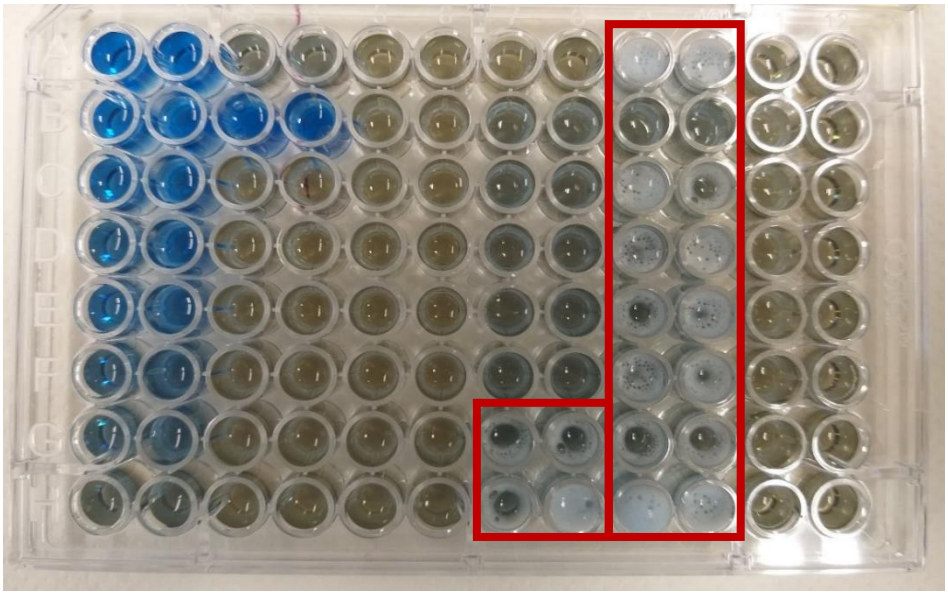

Figure 19 - 96-well plate used for the execution of the Bradford protein assay. In red is marked the samples that reacted with the Coomassie solution. All marked samples contained magnetite MNPs.

Analysing the results from Table 4, the protein concentration remains almost equal among all the samples corresponding to bacteriophage, with the exception of the sample incubated for 20 minutes. However, since this pattern is not seen in any other sample, this result can be attributed to errors from the operator. Also, when comparing to the protein concentration obtained for the T7 phage control, it is also possible to observe that there is no difference between the values, leading to conclude that there was no alteration in the protein structure of the phages provoked by the osmotic shock. When observing the results obtained for the samples with particles added before the osmotic treatment, there is an overall significant decrease in protein concentration when compared with the samples with phage only. When compared to the control containing phage only, the same observation can be made, obtaining an average loss of protein content of 54.57%. However, when comparing this samples with the control corresponding to the bacteriophage with MNPs, the same values can be encountered. When observing the results obtained for the samples with particles added after the osmotic shock, an overall decrease in protein concentration can also be found when compared to the samples with phage only. When comparing with the control corresponding to phage only, there's an average loss of protein content of 27.63%, not being as significant as the one reported in the samples with MNPs added before the treatment. However, since the particles reacted with the colorimetric reagent, there is still a possibility of the protein concentrations obtained not corresponding to the real values. Because of this problem, it is possible to conclude that the Bradford Protein Assay is not the best characterization method to be used in this scenario.

5.1.1.2. Magnetic Separation and characterization of Phage-MNPs conjugates

To verify if the phages where magnetized, meaning conjugated with the added MNPs, the samples with MNPs added to the phage solution before and after performing the osmotic treatments were submitted do magnetic separation. Initially only two washes with 5 mL of SM buffer were performed on all samples, storing the supernatant at 4ºC, and an aliquot of 100uL was taken of the magnetic pellet for titration, as to be seen later. However, it was decided to increase the number of washes with the objective of not only ascertain if the phage concentration decreased significantly with the washes and if the phage concentration was maintained between the first collected magnetic pellet and the final obtained one, being possible indicators of the presence of magnetized bacteriophages. Then, two additional washes were performed on the samples with the same volume used previously of SM buffer, storing the supernatant at 4ºC. The magnetic pellet was also stored at 4ºC.
With the objective of characterizing the magnetic separated samples (washes and magnetic pellet), a phage titration was performed according to the previously mentioned protocols. Again, as control, it was used a sample containing 500 µL of T4 bacteriophage with 10mg of magnetite MNPs diluted in 50 mL of autoclaved water and submitted to the same protocol of magnetic separation. Again, the calculation of the obtained PFU/mL was made using equation 1 and only plaques with plaque unit count of 30-300 were used for the calculation to ensure the reliability of the method. The results are presented in Tables 8.2 to 8.5 present in the Attatchments. The number of infectious phage particles present in solution was also calculated for each sample, shown in Tables 5 to 8. When analysing the results obtained in Table

5 corresponding to the samples with phage and MNPs added before performing the osmotic shock, it is possible to see a decrease of more than 90% of the number of infectious phages from the sample before the magnetic separation to the pellet, where more than 90% of the phages stayed in the supernatant. Regarding the results for the magnetic pellet obtained at the end of the first two washes, it is visible a slight increase in the number of infectious phages along the incubation times. When increasing the number of washes, results presented in Table 6, it is possible to observe a decrease in the number of infectious phages at all incubation times from the second to the third wash. When comparing the results from the first obtained pellet to the second, it should be expected a decrease in the number of phages with the number of washes, as observed in the control. However, when comparing the pellets from Table 5 and Table 6, it is possible to see that all incubation times, with the exception of 15 minutes and 30 minutes where the number of infectious phages decreased 97% and 95% respectively, the number of infectious phages is maintained. As for the results for samples corresponding to the condition of the addition of MNPs after the osmotic shock represented in Table 7, similar results are observed. When comparing the results from the pellet to the number of infectious phages that where in the sample before the magnetic separation, it's possible to see a reduction of more than 90% of the number of infectious phages in the magnetic pellet, where the majority of phages remained in the supernatant. Regarding the results for the magnetic pellet obtained at the end of the first two washes, the number of infectious phages is maintained along the incubation times. When increasing the number of washes, results presented in Table 8, it is possible to observe a significant decrease in the number of infectious phages from the third wash to the fourth wash, which should be expected since more phages have been removed in the previous washes. However, when comparing with the control, the magnitude of the obtained values is two times lower than the obtained for the control. When comparing the results from the first obtained pellet to the second, it is possible to observe an average loss of 99.44% of infectivity from the first pellet to the second, which is consistent with the results observed in the control. This could lead to believe that when submitting the phages and the MNPs to osmotic shock, simultaneously, it could lead to the magnetization of the T4 phages, which could explain the maintenance of the number of infectious phages with the washes. However, the same treatment with the MNPs added after could not promote the magnetization of the phages, leading to the loss of infectious phages along washing steps. It is also worth mentioning that, in case of magnetization, only a small portion of phages was conjugated. Remaining in that hypothesis, this small number of magnetized phages could be due to the mass of MNPs added is not enough for the number of phages in solution. The best way to validate these hypotheses is through the obtention of images in TEM, being the characterization method chosen to perform next.

5.1.1.3. TEM

TEM was used to the characterization of native and treated phages, and to localize the magnetic nanoparticles on the phage. Samples corresponding to 20 and 30 minutes of salt incubation with MNPs added before the osmotic shock were chosen for visualization. The T4 phage solution and a sample with T4 phage solution with added MNPs in suspension were also chosen for visualization for the characterization of the native T4 phage and MNPs. As mentioned previously, Uranyless was used as a negative staining agent in substitution for uranyl acetate, being a safer and less waste making option. The protocol described in 4.7.3 was followed and the obtained images are shown in Figure 20.

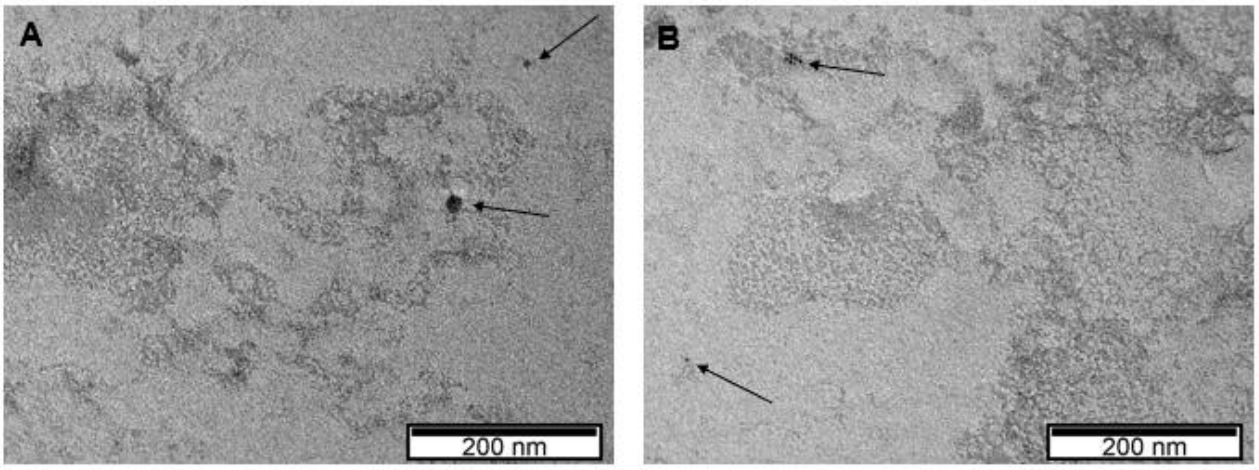

Figure 20 - Obtained TEM visualizations with Uranyless used as negative staining agent. Images **(A)** and **(B)** correspond to the sample with T4 bacteriophage with MNPs added before osmotic shock incubated for 20 minutes. The capture of MNPs agglomerates is marked with arrows.

Images for the native T4 phage and the MNPs were not possible to obtained, not being possible to visualize in TEM (results not shown). A probable cause for this occurrence is the dilution being to high to capture the phage and MNPs in the grid. In further TEM visualizations, the best option is to use non-diluted samples. Observing both Figure 20.A and Figure 20.B, T4 bacteriophages images were not captured, not being possible to verify the location of MNPs on the inside of the phage capsid. However, as identified in both figures, agglomerates of MNPs are shown. The particles appear to have around 4 nm of diameter, confirming to be much smaller than the T4 phage capsid, reported in literature to be 120 nm long and 80 nm wide, as mentioned previously. It is possible that, due to the performance of osmotic shock and the magnetic separation, the phages were too diluted for visualization. In the future, the samples should be concentrated before visualization to try to overcome this problem. However, some type of reaction appears to have taken place, possibly affecting the visualization of the samples.

Table 5 - Osmotic Shock magnetic separation for the condition of particles added before the osmotic shock. Number of phages with infection capacity for each collected fractions till the 2nd washing step in each incubation time.

Phage + Particles (Added Before the Osmotic Shock)						
	Phage Without Particles	Before Separation	Supernatant	1st Wash	2nd Wash	Pellet
Control	-	1.43E+10	1.29E+11	5.65E+08	6.70E+07	>1.50E+08
5	2.15E+09	8.50E+09	1.05E+10	8.60E+08	2.25E+08	2.70E+07
10	1.64E+10	9.05E+09	1.15E+10	8.75E+07	1.29E+08	2.90E+07
15	7.60E+09	8.15E+09	1.60E+10	>1.50E+09	1.55E+08	1.89E+08
20	4.05E+09	8.80E+09	7.50E+09	1.18E+09	2.06E+08	1.53E+08
30	3.40E+09	7.60E+09	1.25E+10	1.07E+10	3.96E+08	4.06E+08

Table 6 - Osmotic Shock magnetic separation for the condition of particles added before the osmotic shock. Number of phages with infection capacity for each all collected fractions in each incubation time.

Phage + Particles (Added Before the Osmotic Shock)								
	Phage Without Particles	Before Separation	Supernatant	1st Wash	2nd Wash	3rd Wash	4th Wash	Pellet
Control	-	1.43E+10	1.29E+11	5.65E+08	6.70E+07	2.03E+08	3.80E+07	6.70E+06
5	2.15E+09	8.50E+09	1.05E+10	8.60E+08	2.25E+08	3.00E+07	2.24E+07	4.69E+07
10	1.64E+10	9.05E+09	1.15E+10	8.75E+07	1.29E+08	5.55E+07	<1.50E+06	>1.50E+08
15	7.60E+09	8.15E+09	1.60E+10	>1.50E+09	1.55E+08	1.53E+08	2.43E+07	6.25E+06
20	4.05E+09	8.80E+09	7.50E+09	1.18E+09	2.06E+08	3.00E+07	2.50E+06	1.55E+08
30	3.40E+09	7.60E+09	1.25E+10	1.07E+10	3.96E+08	7.25E+07	4.50E+06	1.93E+07

Table 7 - Osmotic Shock magnetic separation for the condition of particles added after the osmotic shock. Number of phages with infection capacity for each collected fractions till the 2nd washing step in each incubation time

	Phage + Particles (Added After the Osmotic Shock)					
	Phage Without Particles	Before Separation	Supernatant	1st Wash	2nd Wash	Pellet
Control	-	1.43E+10	1.29E+11	5.65E+08	6.70E+07	1.50E+08
5	2.15E+09	5.65E+10	1.82E+11	>1.50E+10	2.25E+08	3.64E+08
10	1.64E+10	9.00E+09	5.90E+10	>1.50E+10	1.29E+08	2.68E+08
15	7.60E+09	0.00E+00	3.20E+09	1.14E+10	1.55E+08	5.25E+08
20	4.05E+09	2.50E+09	8.00E+09	>1.50E+10	2.06E+08	4.86E+08
30	3.40E+09	1.00E+09	4.00E+10	>1.50E+10	3.96E+08	1.29E+08

Table 8 - Osmotic Shock magnetic separation for the condition of particles added after the osmotic shock. Number of phages with infection capacity for each all collected fractions in each incubation time.

	Phage + Particles (Added After the Osmotic Shock)							
	Phage Without Particles	Before Separation	Supernatant	1st Wash	2nd Wash	3rd Wash	4th Wash	Pellet
Control	-	1.43E+10	1.29E+11	5.65E+08	6.70E+07	2.03E+08	3.80E+07	6.70E+06
5	2.15E+09	5.65E+10	1.82E+11	>1.50E+10	2.25E+08	<1.50E+08	5.00E+05	1.50E+06
10	1.64E+10	9.00E+09	5.90E+10	>1.50E+10	1.29E+08	<1.50E+08	7.00E+05	1.65E+06
15	7.60E+09	0.00E+00	3.20E+09	1.14E+10	1.55E+08	<1.50E+08	3.00E+05	<1.50E+06
20	4.05E+09	2.50E+09	8.00E+09	>1.50E+10	2.06E+08	<1.50E+08	7.50E+05	<1.50E+06
30	3.40E+09	1.00E+09	4.00E+10	>1.50E+10	3.96E+08	<1.50E+08	4.00E+05	<1.50E+06

5.1.2. Sonication

Sonication is a physical method of disruption used in a variety of biological entities. In regards of application in bacteriophages, one of the most common uses of sonication is in the disaggregation of this biological entities in solution. However, in an article published by Machida *et. al*, it was used sonication as a capsid disruption method for the liberation of a coliphage-associated sialidase[88]. So, sonication was proposed as a method for the conjugation of the magnetite MNPs inside the T4 phage capsid. A bath sonication was first proposed since the sonication conditions would be less harsh than the direct sonication provided by a probe sonicator, having less probability of completely disrupting the capsid and only permeabilizing it enough to allow the internalization of the particles. Samples of 1 mL of phage solution and two samples with 1 mL of phage solution with 20 mg of magnetite MNPs where sonicated at 45 kHz and five different times of exposure where tested – 15, 20, 30, 40 and 60 minutes. The temperature increase along the exposure time was also measured, resulting in a temperature of 15.5ºC, 17.8ºC, 23.3ºC, 27.7ºC and 36.0ºC for 15, 20, 30, 40 and 60 minutes of sonication exposure time, respectively. After sonication, samples containing MNPs where magnetically separated according to the procedure described in 4.6.2.

5.1.2.1.1. Bacteriophage Characterization

5.1.2.1.1.1. Samples Titration

As in earlier experimental steps, phage titration was performed as a method for characterizing the magnetic separated samples. As controls, it was used a sample containing 1 mL of T4 bacteriophage with 20mg of magnetite MNPs, submitted to the same protocol of magnetic separation, the samples with 1 mL of phage solution sonicated at each exposition time. Also, as done in previous titration steps, the calculation of the obtained PFU/mL was made using equation 1 and only plates with plaque unit count of 30-300 were used for the calculation to ensure the reliability of the method. The results are presented in Table 9. Since the volume of phage sample for all fractions is of 1 mL, the values obtained in PFU/mL will be the same when converting to number of phages. When comparing the values of the samples with phage with the values obtained for the solution with phage and MNPs before being submitted to sonication to their initial phage concentration – 2.86×10^{10} PFU/mL – it's visible that no lytic activity was lost, meaning that the phages integrity was maintained. In addition, is possible to see an increase in the phage concentration with the sonication exposure time. A possible justification for these results is the decrease on the number of phage aggregates in solution. In an experiment reported by Machida *et. al*, after the sonication of MS2 phage suspension, an increase in the phage number in solution was reported[88]. The authors associated the increase to the reduction of the small phage clusters present in solution.

Table 9 - Bath sonication magnetic separation. Phage concentration in PFU/mL for each all collected fractions in each incubation time.

	Phage Without Particles	Before Separation	Supernatant	1st Wash	2nd Wash	3rd Wash	4th Wash	Pellet
Control	-	2.00E+10	2.00E+09	2.20E+08	< 3.00E+08	1.80E+09	2.70E+09	5.30E+07
t15	1.10E+10	1.40E+10	1.20E+10	6.00E+08	< 3.00E+10	> 3.00E+09	> 3.00E+09	> 3.00E+07
t20	1.20E+10	9.00E+09	7.00E+09	> 3.00E+10	2.16E+09	1.19E+08	1.37E+08	> 3.00E+07
t30	4.30E+10	7.20E+10	2.20E+10	1.90E+09	9.70E+08	< 3.00E+09	< 3.00E+09	2.98E+08
t40	3.55E+11	> 3.00E+11	3.03E+11	1.94E+09	1.91E+10	3.00E+10	1.33E+10	> 3.00E+08
t60	1.86E+11	> 3.00E+11	2.06E+11	8.50E+09	6.10E+09	2.26E+10	1.71E+10	> 3.00E+08

The same increase in the phage concentration can be observed in the supernatant and among the four performed washes, resulting in an increase of up to one magnitude value with the sonication exposure time. When treating the obtained titration results from the pellet, the concentrations from incubation times 15, 20, 40 and 60 minutes where not possible to calculate due to otaining plaque countings out of the 30-300 range necessary for the reliability of the method. However, when observing the plaques from 30, 40 and 60 minutes of exposure time shown in Figure 20, it's possible to see a gradual increase in the number of plaque forming units.

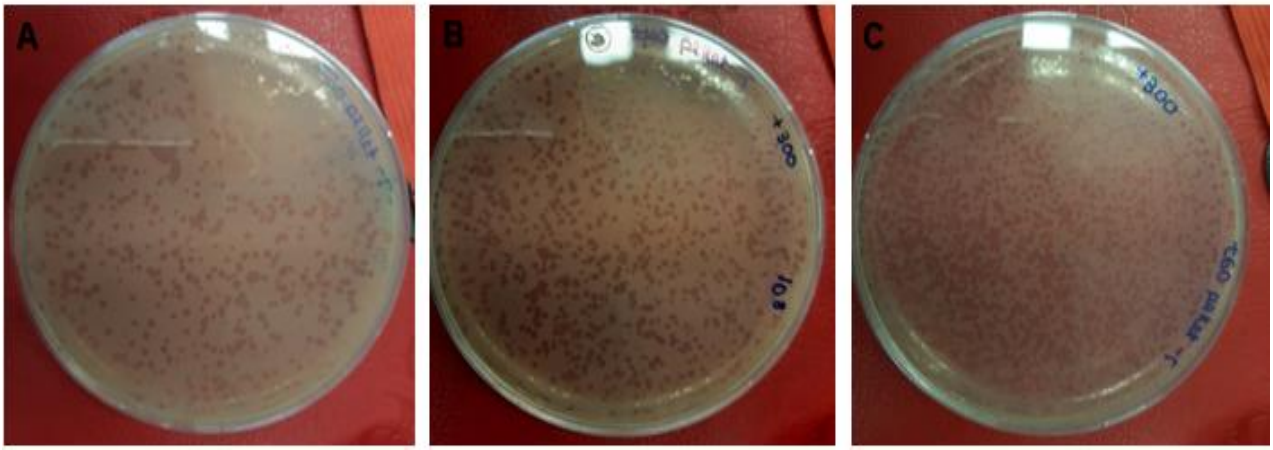

Figure 21 - Plaque forming units for the magnetic pellets of the samples containing T7 bacteriophage with MNPs at different exposure times of sonication. **A-** Sample submitted to 30 minutes of exposure time; **B-** Sample submitted to 40 minutes of exposure time; **C-** Sample submitted to 60 minutes of exposure time.

This gradual increase in the phage concentration with the exposure time can be justified with the decrease of phage agglomerates in solution, leading to a higher number of phages in the pellet. However, this increase can also be due to the possible magnetization of the phages. However, such magnetization can be due to the internalization of the MNPs or to the adsorption of the particles to the exterior of the phage capsid. This hypothesis can only be confirmed when submitting the pellet samples to TEM image capture.

6. Conclusions and Future Work

Bacteriophages have available a wide range of interesting properties that are desirable for the detection of pathogenic bacteria. On the other hand, magnetic nanoparticles present unique properties that, conjugated with bacteriophages, could unravel novel properties for the application of bacterial detection. The main objective of this project is the development and optimization of a conjugation process to obtain magnetic phages. Since the objective of this thesis is the internalization of the MNPs into the bacteriophage capsid, methods that could possibly permeabilize the capsid were chosen. Both results from the osmotic shock and bath sonication where not conclusive in regard to the efficiency of the processes in the conjugation of the particles. The characterization tests should be repeated, with the optimization of the uranyless staining protocol for TEM visualization. However, in the future, some other conjugation methods and conditions would be applied. Since in the chemical treatment used did not totally diminished the lytic activity of the phages, is probable that the conditions used were not enough to completely destabilize the protein capsid of the T4 bacteriophages, but it could be enough to lead to the creation of gaps that would allow the release of DNA and possibly the internalization of bacteriophages. Additionally, Anderson *et. al* reported that when submitting suspensions of T2, T4 and T6 (large virus) phages to high concentrations of salt and then quickly diluted, the phages lost infectivity capacity and the presence of "ghost" phages in solution. However, interestingly, the authors also reported that when submitting suspensions of T1, T3, T5 and T7 (small virus) to the same conditions, they kept their capacity of infection and appeared to remain intact[106]. Jurczak-Kurek *et al.*, as a method to study the morphological and biological properties of a wide group of bacteriophages isolated from urban sewage, proceeded to submit the phages to osmotic shock conditions (same conditions as the protocol used in the article by Anderson *et al.*). The authors reported that from 83 phages tested, 21 where susceptible to osmotic shock, where 18 of them presented larger capsid size compared to the rest and belonging to the *Myoviridae*[107]. T4 is described in literature as having a 120 nm long and 86 nm wide icosahedral capsid[108], confirming to be much larger than odd-numbered phages, like a T7 phage, which is described as a much smaller phage, having a capsid around 60 nm wide[109]. So, in the future, it should also be taken into account the size of the bacteriophages, since it appears that larger bacteriophages appear to be more susceptible to osmotic shock conditions than smaller phages. With this in mind, different phages with different sizes should be submitted to the same treatments. Also, higher salt concentrations (e.g. 5M and 6M) should also be tested. Another chemical method could also be tested as conjugation method, such as alkaline treatment. Liu *et. al*. reported the obtention of "ghost" phages when submitting them to an alkaline treatment, proving to destabilize the protein capsid to remove the phage DNA[57]. However, the applied conditions are not reported by the authors. On the other hand, Muller-Salamin *et. al*. reported the obtention of gaps or openings in T4 capsid when submitting them to a treatment of pH 11.0 in 7M of urea[110]. These small gaps could allow the entrance of the MNPs, magnetizing the phages. Even though this protocol was only tested in capsids and not the whole phage, the maintaining of the tail components would need to also be evaluated. Regarding the results from bath sonication, they were not conclusive, especially since TEM visualization was also not possible. So the repetition of the test would be needed. However, different temperatures could be tested to promote

the capsid proteins denaturation, which could increase the probability of the internalization of the MNPs. Probe sonication would also be tested and compared to the results obtained for bath sonication, since the application of the ultrasounds it's directly applied into the sample, leading to a bigger disruption of the capsid and possibly causing more movement of the magnetic particles and "pushing" the MNPs into the interior of the capsid. The efficiency of the techniques and characterization of the bacteriophages will be evaluated through TEM with the new staining agent. To further evaluate the validation and detection of the magnetic phages, magnetoresistive sensors developed by INESC-MN would be used. This sensor is composed by two distinct sensing areas arranged in two columns, each being composed by 3 groups of 5 U-shaped 2.5x80 μm^2 spin-valve sensors. One of the sensors has no phage probe attached, functioning as a reference. The probe sites on the biochip terminate with exposed Cr/Au pads with magnetoresistive sensors underneath, which will detect the magnetic nanoparticles. In Fernandes *et. al*, the magnetoresistive-biochip (MR-Biochip) functionalization was described[55]. In this biochip, phages specific for the target bacteria (in that case Salmonella-specific phages) are spotted over the left column of sensors, while on the right column are non-specific phages for the target. After the introduction of the solution to be tested, the bacteria that are specific for the bacteriophage will be bound, while the unbound cells are washed. Then antibody-conjugated magnetic nanoparticles (MNPs) are introduced, forming a "sandwich" (Figure 10). The number of cells bound to the sensor surface is given by the difference between the signal acquired after washing the unbound MNPs and the baseline signal ($\Delta V_{binding}$). However, for the testing of the developed magnetic-phages, they would be the substitute for the antibody-conjugated MNPs. The main finality of the produced magnetic-phages is to be used in the development of magnetic-based detection assays.

7. References

1. Sengupta, S., Chattopadhyay, M. K. & Grossart, H. P. The multifaceted roles of antibiotics and antibiotic resistance in nature. *Frontiers in Microbiology* **4**, (2013).

2. Maugeri, G., Lychko, I., Sobral, R. & Roque, A. C. A. Identification and Antibiotic-Susceptibility Profiling of Infectious Bacterial Agents: A Review of Current and Future Trends. *Biotechnol. J.* **14**, 1700750 (2019).

3. Alanis, A. J. Resistance to antibiotics: Are we in the post-antibiotic era? *Archives of Medical Research* **36**, 697–705 (2005).

4. Farooq, U., Wajid Ullah, M., Yang, Q. & Wang, S. Applications of Phage-Based Biosensors in the Diagnosis of Infectious Diseases, Food Safety, and Environmental Monitoring. in *Biosensors for Environmental Monitoring* (IntechOpen, 2019). doi:10.5772/intechopen.88644

5. Ahmed, A., Rushworth, J. V., Hirst, N. A. & Millner, P. A. Biosensors for whole-cell bacterial detection. *Clin. Microbiol. Rev.* **27**, 631–646 (2014).

6. Farooq, U., Yang, Q., Wajid Ullah, M. & Wang, S. Principle and Development of Phage-Based Biosensors. in *Biosensors for Environmental Monitoring* (IntechOpen, 2019). doi:10.5772/intechopen.86419

7. Richter, Ł., Janczuk-Richter, M., Niedziółka-Jönsson, J., Paczesny, J. & Hołyst, R. Recent advances in bacteriophage-based methods for bacteria detection. *Drug Discovery Today* **23**, 448–455 (2018).

8. Allegranzi, B. *et al.* Burden of endemic health-care-associated infection in developing countries: Systematic review and meta-analysis. *Lancet* **377**, 228–241 (2011).

9. Buzby, J. C. & Roberts, T. The Economics of Enteric Infections: Human Foodborne Disease Costs. *Gastroenterology* **136**, 1851–1862 (2009).

10. Farooq, U., Yang, Q., Ullah, M. W. & Wang, S. Bacterial biosensing: Recent advances in phage-based bioassays and biosensors. *Biosensors and Bioelectronics* **118**, 204–216 (2018).

11. Roque, A. C. A., Lowe, C. R. & Taipa, M. Â. Antibodies and genetically engineered related molecules: Production and purification. *Biotechnology Progress* **20**, 639–654 (2004).

12. Ahmed, M. U., Zourob, M. & Tamiya, E. *Immunosensors*. (Royal Society of Chemistry, 2019).

13. Banica, F.-G. *Chemical sensors and biosensors : fundamentals and applications*. (John Wiley & Sons Inc, 2012).

14. Bănică, F. G. *Chemical Sensors and Biosensors: Fundamentals and Applications*. *Chemical Sensors and Biosensors: Fundamentals and Applications* (John Wiley and Sons, 2012). doi:10.1002/9781118354162

15. Alocilja, E. & Muhammad-Tahir, Z. Label-Free Microbial Biosensors Using Molecular Nanowire Transducers. in *Principles of Bacterial Detection: Biosensors, Recognition Receptors and Microsystems* 377–413 (Springer New York, 2008). doi:10.1007/978-0-387-75113-9_16

16. Ho, R. J. Y. & Gibaldi, M. Antibodies and Derivatives. in *Biotechnology and Biopharmaceuticals* 271–311 (John Wiley & Sons, Inc., 2004). doi:10.1002/0471704210.ch10

17. Morales, M. A. & Halpern, J. M. Guide to Selecting a Biorecognition Element for Biosensors. *Bioconjug. Chem.* **29**, 3231–3239 (2018).

18. Lara, S. & Perez-Potti, A. Applications of nanomaterials for immunosensing. *Biosensors* **8**, 104 (2018).

19. Dover, J. E., Hwang, G. M., Mullen, E. H., Prorok, B. C. & Suh, S. J. Recent advances in peptide probe-based biosensors for detection of infectious agents. *Journal of Microbiological Methods* **78**, 10–19 (2009).

20. Tawil, N., Sacher, E., Mandeville, R. & Meunier, M. Bacteriophages: Biosensing tools for multi-

drug resistant pathogens. *Analyst* **139**, 1224–1236 (2014).

21. Saerens, D., Huang, L., Bonroy, K. & Muyldermans, S. Antibody fragments as probe in biosensor development. *Sensors* **8**, 4669–4686 (2008).

22. Yu, X. *et al.* Nanobodies derived from Camelids represent versatile biomolecules for biomedical applications. *Biomaterials Science* **8**, 3559–3573 (2020).

23. Zhou, W., Jimmy Huang, P. J., Ding, J. & Liu, J. Aptamer-based biosensors for biomedical diagnostics. *Analyst* **139**, 2627–2640 (2014).

24. Han, K., Liang, Z. & Zhou, N. Design Strategies for Aptamer-Based Biosensors. *Sensors* **10**, 4541–4557 (2010).

25. Lakhin, A. V, Tarantul, V. Z. & Gening, L. V. *Aptamers: Problems, Solutions and Prospects*. *34* | *ActA nAturAe* | **5**, (2013).

26. Yang, S. *et al.* Oligonucleotide Aptamer-Mediated Precision Therapy of Hematological Malignancies. *Molecular Therapy - Nucleic Acids* **13**, 164–175 (2018).

27. Sharma, S. *et al.* Bacteriophages and its applications: an overview. *Folia Microbiol. (Praha).* **62**, 17–55 (2017).

28. Casey, A., Coffey, A. & McAuliffe, O. Genetics and Genomics of Bacteriophages. in *Bacteriophages* 1–26 (Springer International Publishing, 2017). doi:10.1007/978-3-319-40598-8_5-1

29. Hungaro, H. M., Lopez, M. E. S., Albino, L. A. A. & Mendonça, R. C. S. Bacteriophage: The Viruses Infecting Bacteria and Their Multiple Applications. in *Reference Module in Earth Systems and Environmental Sciences* (Elsevier, 2014). doi:10.1016/b978-0-12-409548-9.09039-4

30. Ertürk, G. & Lood, R. Bacteriophages as biorecognition elements in capacitive biosensors: Phage and host bacteria detection. *Sensors Actuators, B Chem.* **258**, 535–543 (2018).

31. Ackermann, H. W. Bacteriophage observations and evolution. *Research in Microbiology* **154**, 245–251 (2003).

32. Kutter, E. & Sulakvelidze, A. *Bacteriophages : biology and applications*. (CRC Press, 2005).

33. Sharp, R. Bacteriophages: biology and history. *J. Chem. Technol. Biotechnol.* **76**, 667–672 (2001).

34. Bruynoghe, R., Maisin, J. & Maisin, J. R. Essais de thérapeutique au moyen du bacteriophage. (1921).

35. Schaechter, M. *Desk encyclopedia of microbiology*. (Elsevier/AcademicPress, 2009).

36. Orlova, E. V. Bacteriophages and Their Structural Organisation. in *Bacteriophages* (InTech, 2012). doi:10.5772/34642

37. Leiman, P. G. & Shneider, M. M. Contractile tail machines of bacteriophages. *Adv. Exp. Med. Biol.* **726**, 93–114 (2012).

38. NSF - OLPA - PR 02-07: NEW UNDERSTANDING OF COMPLEX VIRUS NANO-MACHINE FOR CELL PUNCTURING AND DNA DELIVERY Images. Available at: https://www.nsf.gov/od/lpa/news/02/pr0207images.htm. (Accessed: 16th January 2020)

39. International Committee on Taxonomy of Viruses (ICTV). Available at: https://talk.ictvonline.org/taxonomy/p/taxonomy_releases. (Accessed: 4th January 2020)

40. Frost, L. S., Leplae, R., Summers, A. O. & Toussaint, A. Mobile genetic elements: The agents of open source evolution. *Nature Reviews Microbiology* **3**, 722–732 (2005).

41. Ackermann, H. W. 5500 Phages examined in the electron microscope. *Archives of Virology* **152**, 227–243 (2007).

42. Azeredo, J. & Sutherland, I. The Use of Phages for the Removal of Infectious Biofilms. *Curr. Pharm. Biotechnol.* **9**, 261–266 (2008).

43. Kurtboke, I. *Bacteriophages*. (InTech, 2012). doi:10.5772/1065

44. Maniloff, J. Bacteriophages. in *Encyclopedia of Life Sciences (ELS)* (John Wiley & Sons, Ltd, 2012). doi:10.1002/9780470015902.a0000773.pub3

45. Harada, L. K. *et al.* Biotechnological applications of bacteriophages: State of the art. *Microbiol. Res.* **212**–**213**, 38–58 (2018).

46. Peltomaa, R., López-Perolio, I., Benito-Peña, E., Barderas, R. & Moreno-Bondi, M. C. Application of bacteriophages in sensor development. *Anal. Bioanal. Chem.* **408**, 1805–1828 (2016).

47. Campbell, A. The future of bacteriophage biology. *Nature Reviews Genetics* **4**, 471–477 (2003).

48. Stone, E., Campbell, K., Grant, I. & McAuliffe, O. Understanding and exploiting phage–host interactions. *Viruses* **11**, 567 (2019).

49. Letarov, A. V. & Kulikov, E. E. Adsorption of bacteriophages on bacterial cells. *Biochemistry (Moscow)* **82**, 1632–1658 (2017).

50. Bertozzi Silva, J., Storms, Z. & Sauvageau, D. Host receptors for bacteriophage adsorption. *FEMS Microbiol. Lett.* **363**, fnw002 (2016).

51. Riede, I. Receptor specificity of the short tail fibres (gp12) of T-even type Escherichia coli phages. *MGG Mol. Gen. Genet.* **206**, 110–115 (1987).

52. Heller, K. & Braun, V. Polymannose O-antigens of Escherichia coli, the binding sites for the reversible adsorption of bacteriophage T5+ via the L-shaped tail fibers. *J. Virol.* **41**, 222–227 (1982).

53. Heller, K. J. Identification of the phage gene for host receptor specificity by analyzing hybrid phages of T5 and BF23. *Virology* **139**, 11–21 (1984).

54. D.V. Rakhuba, E.I. Kolomiets, E Szwajcer Dey & G.I. Novik. Bacteriophage Receptors, Mechanisms of Phage Adsorption and Penetration into Host Cell. *Polish J. Microbiol.* (2010).

55. Fernandes, E. *et al.* A bacteriophage detection tool for viability assessment of Salmonella cells. *Biosens. Bioelectron.* **52**, 239–246 (2014).

56. Liu, C. M., Jin, Q., Sutton, A. & Chen, L. A novel fluorescent probe: Europium complex hybridized T7 phage. *Bioconjug. Chem.* **16**, 1054–1057 (2005).

57. Liu, C. *et al.* Magnetic viruses via nano-capsid templates. *J. Magn. Magn. Mater.* **302**, 47–51 (2006).

58. Lee, B. K., Yun, Y. H. & Park, K. Smart nanoparticles for drug delivery: Boundaries and opportunities. *Chem. Eng. Sci.* **125**, 158–164 (2015).

59. Issa, B., Obaidat, I., Albiss, B. & Haik, Y. Magnetic Nanoparticles: Surface Effects and Properties Related to Biomedicine Applications. *Int. J. Mol. Sci.* **14**, 21266–21305 (2013).

60. Martins, V. C. *et al.* Challenges and trends in the development of a magnetoresistive biochip portable platform. *J. Magn. Magn. Mater.* **322**, 1655–1663 (2010).

61. Giouroudi, I. & Keplinger, F. Microfluidic Biosensing Systems Using Magnetic Nanoparticles. *Int. J. Mol. Sci.* **14**, 18535–18556 (2013).

62. Steckiewicz, K. P. & Inkielewicz-Stepniak, I. Modified nanoparticles as potential agents in bone diseases: Cancer and implant-related complications. *Nanomaterials* **10**, 658 (2020).

63. Kodama, R. H. Magnetic nanoparticles. *J. Magn. Magn. Mater.* **200**, 359–372 (1999).

64. Hasanzadeh, M., Shadjou, N. & de la Guardia, M. Iron and iron-oxide magnetic nanoparticles

as signal-amplification elements in electrochemical biosensing. *TrAC - Trends in Analytical Chemistry* **72**, 1–9 (2015).

65. Xu, J. *et al.* Application of iron magnetic nanoparticles in protein immobilization. *Molecules* **19**, 11465–11486 (2014).

66. Jazayeri, M. H., Amani, H., Pourfatollah, A. A., Pazoki-Toroudi, H. & Sedighimoghaddam, B. Various methods of gold nanoparticles (GNPs) conjugation to antibodies. *Sensing and Bio-Sensing Research* **9**, 17–22 (2016).

67. Jin, Y., Liu, F., Shan, C., Tong, M. & Hou, Y. Efficient bacterial capture with amino acid modified magnetic nanoparticles. *Water Res.* **50**, 124–134 (2014).

68. Sinatra, F. Understanding the Interaction Between Blood Flow and an Applied Magnetic Field. *Grad. Theses Diss.* (2010).

69. Akbarzadeh, A., Samiei, M. & Davaran, S. Magnetic nanoparticles: Preparation, physical properties, and applications in biomedicine. *Nanoscale Res. Lett.* **7**, 1–13 (2012).

70. Figuerola, A., Di Corato, R., Manna, L. & Pellegrino, T. From iron oxide nanoparticles towards advanced iron-based inorganic materials designed for biomedical applications. *Pharmacological Research* **62**, 126–143 (2010).

71. Enriquez-Navas, P. M. & Garcia-Martin, M. L. Application of inorganic nanoparticles for diagnosis based on MRI. in *Frontiers of Nanoscience* **4**, 233–245 (Elsevier Ltd, 2012).

72. Marghussian, V. Magnetic Properties of Nano-Glass Ceramics. in *Nano-Glass Ceramics* 181–223 (Elsevier, 2015). doi:10.1016/b978-0-323-35386-1.00004-9

73. Ramanujan, R. V. Magnetic particles for biomedical applications. in *Biomedical Materials* 477–491 (Springer US, 2009). doi:10.1007/978-0-387-84872-3_17

74. Wang, L. & Lin, J. Recent advances on magnetic nanobead based biosensors: From separation to detection. *TrAC - Trends in Analytical Chemistry* **128**, 115915 (2020).

75. Issadore, D. *et al.* Magnetic sensing technology for molecular analyses. *Lab Chip* **14**, 2385–2397 (2014).

76. Shevtsov, M., Zhao, L., Protzer, U. & Klundert, M. Applicability of Metal Nanoparticles in the Detection and Monitoring of Hepatitis B Virus Infection. *Viruses* **9**, 193 (2017).

77. Koh, I. & Josephson, L. Magnetic Nanoparticle Sensors. *Sensors* **9**, 8130–8145 (2009).

78. Xianyu, Y., Wang, Q. & Chen, Y. Magnetic particles-enabled biosensors for point-of-care testing. *TrAC - Trends in Analytical Chemistry* **106**, 213–224 (2018).

79. Pappert, G., Rieger, M., Niessner, R. & Seidel, M. Immunomagnetic nanoparticle-based sandwich chemiluminescence-ELISA for the enrichment and quantification of E. coli. *Microchim. Acta* **168**, 1–8 (2010).

80. Cheng Y, F. Biosensors for Bacterial Detection. *Int. J. Biosens. Bioelectron.* **2**, (2017).

81. Dhull, V., Gahlaut, A., Dilbaghi, N. & Hooda, V. Acetylcholinesterase biosensors for electrochemical detection of organophosphorus compounds: A review. *Biochem. Res. Int.* (2013). doi:10.1155/2013/731501

82. Evtugyn, G. Biosensor Signal Transducers. in 99–205 (2014). doi:10.1007/978-3-642-40241-8_3

83. Huang, H. T. *et al.* Magnetoresistive Biosensors for Direct Detection of Magnetic Nanoparticle Conjugated Biomarkers on a Chip. *SPIN* **09**, 1940002 (2019).

84. Su, D., Wu, K., Saha, R., Peng, C. & Wang, J. P. Advances in magnetoresistive biosensors. *Micromachines* **11**, (2020).

85. Martins, V. C. *et al.* Femtomolar limit of detection with a magnetoresistive biochip. *Biosens. Bioelectron.* **24**, 2690–2695 (2009).

86. Binasch, G., Grünberg, P., Saurenbach, F. & Zinn, W. Enhanced magnetoresistance in layered magnetic structures with antiferromagnetic interlayer exchange. *Phys. Rev. B* **39**, 4828–4830 (1989).

87. Baibich, M. N. *et al.* Giant magnetoresistance of (001)Fe/(001)Cr magnetic superlattices. *Phys. Rev. Lett.* **61**, 2472–2475 (1988).

88. Machida, Y. *et al.* Structure and function of a novel coliphage-associated sialidase. *FEMS Microbiol. Lett.* **182**, 333–337 (2000).

89. Ramli, R., Haryanto, F., Khairurrijal, K. & Djamal, M. GMR Biosensors for Clinical Diagnostics. in *Biosensors for Health, Environment and Biosecurity* (InTech, 2011). doi:10.5772/16365

90. Cao, B. *et al.* Development of magnetic sensor technologies for point-of-care testing: Fundamentals, methodologies and applications. *Sensors and Actuators, A: Physical* **312**, 112130 (2020).

91. Baselt, D. R. *et al.* A biosensor based on magnetoresistance technology. *Biosens. Bioelectron.* **13**, 731–739 (1998).

92. Li, Y. *et al.* Nanomagnetic competition assay for low-abundance protein biomarker quantification in unprocessed human sera. *J. Am. Chem. Soc.* **132**, 4388–4392 (2010).

93. Freitas, P. P. *et al.* Spintronic platforms for biomedical applications. *Lab on a Chip* **12**, 546–557 (2012).

94. Romao, V. C. *et al.* Lab-on-Chip Devices: Gaining Ground Losing Size. *ACS Nano* **11**, 10659–10664 (2017).

95. Nabaei, V., Chandrawati, R. & Heidari, H. Magnetic biosensors: Modelling and simulation. *Biosens. Bioelectron.* **103**, 69–86 (2018).

96. Freitas, P. P., Ferreira, R., Cardoso, S. & Cardoso, F. Magnetoresistive sensors. *J. Phys. Condens. Matter* **19**, 165221 (2007).

97. Parkin, S. S. P. *et al.* Giant tunnelling magnetoresistance at room temperature with MgO (100) tunnel barriers. *Nat. Mater.* **3**, 862–867 (2004).

98. Shen, W., Liu, X., Mazumdar, D. & Xiao, G. In situ detection of single micron-sized magnetic beads using magnetic tunnel junction sensors. *Appl. Phys. Lett.* **86**, 1–3 (2005).

99. Germano, J. *et al.* A Portable and Autonomous Magnetic Detection Platform for Biosensing. *Sensors* **9**, 4119–4137 (2009).

100. Wu, Y., Liu, Y., Zhan, Q., Liu, J. P. & Li, R. W. Rapid detection of Escherichia coli O157:H7 using tunneling magnetoresistance biosensor. *AIP Adv.* **7**, 056658 (2017).

101. Sun, W., Brovko, L. & Griffiths, M. Use of bioluminescent Salmonella for assessing the efficiency of constructed phage-based biosorbent. *J. Ind. Microbiol. Biotechnol.* **27**, 126–128 (2001).

102. Bennett, A. R., Davids, F. G. C., Vlahodimou, S., Banks, J. G. & Betts, R. P. The use of bacteriophage-based systems for the separation and concentration of Salmonella. *J. Appl. Microbiol.* **83**, 259–265 (1997).

103. Liébana, S. *et al.* Phagomagnetic Separation and Electrochemical Magneto-Genosensing of Pathogenic Bacteria. *Anal. Chem.* **85**, 3079–3086 (2013).

104. Chen, J. *et al.* Bacteriophage-based nanoprobes for rapid bacteria separation. *Nanoscale* **7**, 16230–16236 (2015).

105. Janczuk, M. *et al.* Bacteriophage-Based Bioconjugates as a Flow Cytometry Probe for Fast Bacteria Detection. *Bioconjug. Chem.* **28**, 419–425 (2017).

106. Anderson, T. F. The reactions of bacterial viruses with their host cells. *Bot. Rev.* **15**, 464–505 (1949).

107. Jurczak-Kurek, A. *et al.* Biodiversity of bacteriophages: Morphological and biological properties of a large group of phages isolated from urban sewage. *Sci. Rep.* **6**, 1–17 (2016).

108. Rao, V. B. & Black, L. W. Structure and assembly of bacteriophage T4 head. *Virology Journal* **7**, 356 (2010).

109. Deng, X., Wang, L., You, X., Dai, P. & Zeng, Y. Advances in the T7 phage display system (Review). *Molecular Medicine Reports* **17**, 714–720 (2018).

110. Muller-Salamin, L., Onorato, L. & Showe, M. K. *Localization of Minor Protein Components of the Head of Bacteriophage T4*. *JOURNAL OF VIROLOGY* (1977).

8. Attachments

8.1. (%) Loss of Infectivity Calculation:

Table 8.1- T4 phage osmotic shock for all tested conditions. Obtained (%) loss of infectivity values for each condition for at incubation times. Negative values are considered has no loss of infectivity.

Incubation Time (min)	Phage Only	Phage + Particles (Before)	Phage + Particles (After)
5 min	85%	41%	-295%
10 min	-15%	37%	37%
15 min	47%	43%	-
20 min	72%	38%	83%
30 min	76 %	47%	93%
Average	70%	41%	71%

8.2. Osmotic Shock Titration Results (PFU/mL):

Table 8.2- Osmotic Shock magnetic separation for the condition of particles added before the osmotic shock. Phage concentration in PFU/mL for each collected fractions till the 2nd washing step in each incubation time.

Phage + Particles (Added Before the Osmotic Shock)						
	Phage Without Particles	Before Separation	Supernatant	1st Wash	2nd Wash	Pellet
Control	-	2.86E+08	2.57E+09	1.13E+09	1.34E+07	>3.00E+07
5	4.30E+07	1.70E+08	2.10E+08	1.72E+09	4.49E+07	5.40E+06
10	3.28E+08	1.81E+08	2.30E+08	1.75E+08	2.58E+07	5.80E+06
15	1.52E+08	1.63E+08	3.20E+08	> 3.00E+09	3.10E+07	3.77E+07
20	8.10E+07	1.76E+08	1.50E+08	2.35E+09	4.13E+07	3.06E+07
30	6.80E+07	1.52E+08	2.50E+08	2.13E+09	7.93E+07	8.12E+07

Table 8.3- Osmotic Shock magnetic separation for the condition of particles added before the osmotic shock. Phage concentration in PFU/mL for each all collected fractions in each incubation time.

Phage + Particles (Added Before the Osmotic Shock)								
	Phage Without Particles	Before Separation	Supernatant	1st Wash	2nd Wash	3rd Wash	4th Wash	Pellet
Control	-	2.86E+08	2.57E+09	1.13E+09	1.34E+07	4.07E+07	7.60E+06	1.34E+06
5	4.30E+07	1.70E+08	2.10E+08	1.72E+09	4.49E+07	6.00E+06	4.49E+06	9.38E+06
10	3.28E+08	1.81E+08	2.30E+08	1.75E+08	2.58E+07	1.11E+07	< 3.00E+05	> 3.00E+07
15	1.52E+08	1.63E+08	3.20E+08	> 3.00E+09	3.10E+07	3.05E+07	4.85E+06	1.25E+06
20	8.10E+07	1.76E+08	1.50E+08	2.35E+09	4.13E+07	6.00E+06	5.00E+05	3.10E+07
30	6.80E+07	1.52E+08	2.50E+08	2.13E+09	7.93E+07	1.45E+07	9.00E+05	3.85E+06

Table 8.4- Osmotic Shock magnetic separation for the condition of particles added after the osmotic shock. Phage concentration in PFU/mL for each collected fractions till the 2nd washing step in each incubation time.

Phage + Particles (Added After the Osmotic Shock)						
	Phage Without Particles	Before Separation	Supernatant	1st Wash	2nd Wash	Pellet
Control	-	2.86E+08	2.57E+09	1.13E+09	1.34E+07	> 3.00E+07
5	4.30E+07	1.13E+09	3.63E+09	> 3.00E+09	1.24E+08	7.28E+07
10	3.28E+08	1.80E+08	1.18E+09	> 3.00E+09	3.80E+07	5.36E+07
15	1.52E+08	0.00E+00	6.40E+07	2.28E+09	8.59E+07	1.05E+08
20	8.10E+07	5.00E+07	1.60E+08	> 3.00E+09	7.39E+07	9.72E+07
30	6.80E+07	2.00E+07	8.00E+08	> 3.00E+09	5.29E+07	2.58E+07

Table 8.5- Osmotic Shock magnetic separation for the condition of particles added after the osmotic shock. Phage concentration in PFU/mL for each all collected fractions in each incubation time.

Phage + Particles (Added After the Osmotic Shock)								
	Phage Without Particles	Before Separation	Supernatant	1st Wash	2nd Wash	3rd Wash	4th Wash	Pellet
Control	-	2.86E+08	2.57E+09	1.13E+09	1.34E+07	4.07E+07	7.60E+06	1.34E+06
5	4.30E+07	1.13E+09	3.63E+09	> 3.00E+09	1.24E+08	< 3.00E+07	1.00E+05	3.00E+05
10	3.28E+08	1.80E+08	1.18E+09	> 3.00E+09	3.80E+07	< 3.00E+07	1.40E+05	3.30E+05
15	1.52E+08	0.00E+00	6.40E+07	2.28E+09	8.59E+07	< 3.00E+07	6.00E+04	< 3.00E+05
20	8.10E+07	5.00E+07	1.60E+08	> 3.00E+09	7.39E+07	< 3.00E+07	1.50E+05	< 3.00E+05
30	6.80E+07	2.00E+07	8.00E+08	> 3.00E+09	5.29E+07	< 3.00E+07	8.00E+04	< 3.00E+05